

Norwegian University  
of Life Sciences

Master's Thesis 2017  
30 ECTS  
Faculty of Science and Technology

# The NMBU Phenotyping Robot; A Modified Version of Thorvald

NMBUs Fenotyperobot; En Modifisert  
Versjon av Thorvald

Kristine Skattum  
Mechanical Engineering







# Preface

Writing a master's thesis has always been a dream to me. My aunt is a civil engineer, and when I was younger she told me a lot about her job and how much she loved it. I have wanted to become an engineer ever since. She inspired me, and that's why I am sitting here today writing my master's thesis. It has been a goal for several years, and now I'm finally here.

Choosing a subject for my thesis was quite hard. I did not know what I wanted at the time, and I was very insecure when I chose the Thorvald project. In my five years at the university, I have only had one robotics class, so this was a step into the unknown. I knew that I wanted to work with design, so when the Thorvald team told me that they had a design project, I couldn't say no. I haven't regretted my decision once.

The robot is requested by Vollebekk research farm. They want a version of Thorvald that can be used for phenotyping. In a meeting with them in December, they told me all the modifications that had to be done to make Thorvald suited for this task.

In January, most of the robotics team, including me, went on a trip to Brazil to visit both a farm and other robotic teams for inspiration. One of the stops was UMOE in Presidente Prudente, which is a "Norwegian" farm in Brazil. With its 400 000 acres of sugarcane, we saw great potential for our robots.

I would like to thank Electro Drives AS and Røwdehjul AS for good service. I would like to thank Bjørn Tenge for validation of design. A big thank you to my fellow master student and friend Rémy Zakaria for help and great teamwork. Thank you Marius Austad and Øystein Tårnes Sund for all the help with design, component selection etc.

Finally, I would like to thank my supervisor Prof. Pål Johan From and his PhD. candidate Lars Grimstad. This thesis would not have been anything without your supervision and guidance.

Ås

11/5-2017

---

Kristine Skattum

# Abstract

Soil compaction is a big problem in farming industry. This is why Pål Johan From in 2014, along with four master students, designed and built the agricultural robot Thorvald I. A light weighted robot that avoids soil compaction. Two years later, a new team of master students designed and built Thorvald II, where the goal was to make the robot module based. The modularity formed the basis of this thesis, where the goal was to design a modified version of Thorvald.

The modified robot is ordered by Vollebekk research farm, and its task is phenotyping, which is the observation of grain health. The goal was to make the robot capable of driving in the research field without causing any damage on grains.

The selections of designs and components are based on Pugh's method. Where different designs and components are compared based on advantages and drawbacks, and the one with the highest score is selected. In addition to designs and components, different materials and assembly techniques have been discussed.

A Tora module was built before this thesis started, and tested in March this year. The test showed promising results, and an analysis was therefore made to find out if a lighter module could be used.

Some modifications had to be made to the Thorvald wheel module to satisfy the requirements set by Vollebekk research farm, but as the changes were small, the modularity requirement was still fulfilled. Covers were designed with Vollebekk research farm's requirements in mind. The goals were to make sure that the cover could separate the grains without damaging them, and still retain Thorvald's modularity. With these requirements in mind, the covers were designed for use on four-wheel drive, four-wheel steering as well as this robot with two-wheel drive and caster wheels with differential steering.

Time was the biggest obstacle in this thesis, and a functioning robot is therefore not tested yet. With the modifications made in mind, the robot will work better than Thorvald did last year. If results from testing look promising, the robot is ready for the phenotyping field. If not, new modifications should be made with following tests.

To obtain optimal functionality, the next version of the robot should implement the following changes;

- Skid steering instead of differential steering
- Use of smaller dimensions on the Tora module, 40 mm pipes

# Sammendrag

Jordkomprimering er et stort problem i landbruksindustrien. I 2014 startet derfor Pål Johan From, i samarbeid med fire mastergradsstudenter, et prosjekt hvor landbruksroboten Thorvald I ble utviklet og bygget. Thorvald I er en lett robot som hindrer jordkomprimering. To år senere utviklet en ny gruppe masterstudenter Thorvald II, hvor målet var å gjøre roboten modulbasert. Modulariteten dannet grunnlaget for denne oppgaven, hvor målet var å designe en modifisert versjon av Thorvald.

Den modifiserte roboten er bestilt av Vollebekk forsøksgård, og dens bruksområde er fenotyping, som er definert som observasjonen av kornhelse. Målet var at roboten skulle kunne kjøre i forskningsfeltet uten å forårsake skader på kornet.

Valgene av design og komponenter er basert på Pughs metode. Ulike design og komponenter sammenlignes basert på fordeler og ulemper, hvor komponenten/designet med høyest poengsum blir valgt. Forskjellige materialer og monterings teknikker diskuteres også i oppgaven.

I forkant av denne oppgaven ble en Tora-modul bygget av et Volvo veltebur. Modulen ble testet i mars 2017, og ga lovende resultater. På bakgrunn av resultatene inneholder oppgaven en analyse for å finne ut om en lettere versjon av modulen kan benyttes.

Det har blitt gjort enkelte endringer på Thorvalds hjulmodul for å tilfredsstille kravene til Vollebekk forsøksgårdsgård. Imidlertid er endringene så små at modulkravet kan sies å være så godt som oppfylt. Dekslene har blitt designet i henhold til forsøksgårdens krav. Målet var å sørge for at dekslet kunne skille kornene uten å skade dem, og samtidig beholde modulariteten. Dekslene er derfor designet for bruk på Thorvald II med firehjulstrekk og firehjulsstyring, og fenotyperoboten med tohjulstrekk og handlevognshjul med differensialstyring.

På grunn av oppgavens tidsbegrensning, gjenstår det fremdeles å teste en fungerende robot. Med endringene tatt i betraktning, vil roboten med sikkerhet fungere bedre enn Thorvald i fjor. Dersom testresultatene er lovende, vil roboten være klar for å benyttes i fenotypefeltet. Hvis ikke bør det foretas nye endringer etterfulgt av nye tester.

For å oppnå optimal funksjonalitet, bør neste versjon av roboten implementere følgende endringer;

- Glidestyring i stedet for differensialstyring
- Bruk av mindre dimensjoner på Tora-modulen, 40 mm rør

# List of Tables

Table 1-1: Overview of requirements with importance .....	4
Table 2-1: Model of a decision matrix with 4 alternatives, 4 criteria, weighting, score(X), weighted score(Y), and weighted sum(Z).....	7
Table 3-1: Solid particle protection .....	19
Table 3-2: Liquid ingress protection.....	20
Table 4-1: Summary of the resistance forces.....	26
Table 5-1: Evaluation of different gears .....	27
Table 5-2: Evaluation of belts and chain .....	28
Table 5-3: Specifications of BL840 .....	30
Table 5-4: Specifications for Apex Dynamics AL110 .....	32
Table 5-5: Pulley specifications.....	33
Table 5-6: Datasheet for the powertrain .....	38
Table 8-1: Test results of the adhesive Araldite AW4858 with hardener HW4858 [50] .....	46
Table 8-2: Evaluation of Covers .....	52
Table 8-3: Evaluation of cover angle.....	53



# List of Figures

Figure 1-1: The agricultural robot Thorvald I.....	1
Figure 1-2: Thorvald II modularity examples. Image: Marius Austad.....	2
Figure 1-3: Thorvald II in a strawberry tunnel. Image: Benjamin Alexander Ward.....	2
Figure 1-4: Thorvald I in the phenotyping field at Vollebekk research farm. Image: NMBU..	3
Figure 1-5: Illustration showing height above ground and angle requirement for the wheel cover.....	4
Figure 2-1: Software logos. (a) SolidWorks, (b) Pages, (c) ANSYS, (d) Microsoft Word, (e) Microsoft Excel.....	8
Figure 3-1: Phenotyping field [7] .....	9
Figure 3-2: Stress-strain diagram [8].....	10
Figure 3-3: Material properties. Specific Stiffness vs. Specific Strength [11] .....	11
Figure 3-4: Metallic Crystal Structures, (a) The face-centered cubic, (b) The body-centered cubic, and (c) The hexagonal close-packed [13] .....	12
Figure 3-5: Rivet (a) before driving, and (b) after driving [20].....	15
Figure 3-6: Ideal vehicle performance characteristics [21] .....	15
Figure 3-7: Brushed DC motor [27].....	16
Figure 3-8: Cross section of a BLDC motor [28].....	17
Figure 3-9: Different gear types. (a) Spur gear, (b) Helical gear, (c) Herringbone gear, (d) Planetary gear [30].....	19
Figure 3-10: (a) Flat belt, (b) V-belt and (c) Circular belt [36] .....	20
Figure 3-11: Timing belts [38].....	21
Figure 4-1: Gradient resistance.....	22
Figure 4-2: Powertrain example.....	24
Figure 4-3: Estimated projection of Tora, front view.....	26
Figure 5-1: Motor and drivetrain example.....	29
Figure 5-2: Picture of 3Men's BL8 series motor [42].....	30

Figure 5-3: Roboteq SBL1360 [43] .....	31
Figure 5-4: Apex Dynamics AL110 planetary gear.....	31
Figure 5-5: Timing belt [44] .....	32
Figure 5-6: Pulleys (a) without flange (b) with flange [44].....	33
Figure 5-7: Caster wheel.....	34
Figure 5-8: (a) Original wheel, (b) Modified wheel and gearbox.....	35
Figure 5-9: Power vs Speed with (a) one wheel locked, and (b) two wheels locked .....	36
Figure 5-10: Simple drawing of the powertrain.....	36
Figure 6-1: Strength test of the Tora module.....	39
Figure 6-2: Illustration of the scenarios analyzed (a) scenario 1, (b) scenario 2 .....	40
Figure 6-3: ANSYS analysis of the Volvo roll cage with scenario 1; (a) Equivalent stress, (b) Total deformation.....	40
Figure 6-4: ANSYS analysis of the Volvo roll cage with scenario 2; (a) Equivalent stress, (b) Total deformation.....	41
Figure 6-5: ANSYS analysis of the lighter cage with scenario 1; (a) Equivalent stress, (b) Total deformation.....	41
Figure 6-6: ANSYS analysis of the lighter cage wit scenario 2; (a) Equivalent stress, (b) Total deformation .....	42
Figure 7-1: (a) Thorvald and (b) Tora wheel module arms .....	43
Figure 7-2: Tora wheel module arm .....	43
Figure 7-3: Tora spacer.....	44
Figure 7-4: Comparison of Thorvald and Tora wheel modules.....	44
Figure 8-1: Curing in a sauna. Image: Remy Zakaria.....	46
Figure 8-2: Test days [50].....	48
Figure 8-3: Covers airplane wheels [51].....	49
Figure 8-4: Round cover .....	49
Figure 8-5: Triangle covers. (a) Three bends, (b) Five bends .....	50

Figure 8-6: Grain harvesting equipment. Image: Kristine Skattum.....	51
Figure 8-7: Illustration of cover with 30 degrees slope .....	51
Figure 8-8: Illustration of cover with 60 degrees slope .....	52
Figure 8-9: Cover parts (a) Wheel module cover, (b) Inside cover, (c) Front cover, and (d) Back cover .....	54
Figure 8-10: Covers (a) Assembled, (b) Exploded view .....	54
Figure 12-1: Construction drawings of the wheel module arm .....	62
Figure 12-2: Construction drawing of the wheel spacer.....	63
Figure 12-3: Construction drawing of the gear axle .....	63
Figure 12-4: Construction drawing of the front cover.....	64
Figure 12-5: Construction drawing of the back cover .....	64
Figure 12-6: Construction drawing of the side cover .....	65
Figure 12-7: Construction drawing of the wheel cover .....	65

# Table of Contents

<b>1</b>	<b>INTRODUCTION</b>	<b>1</b>
1.1	THE THORVALD PROJECT	1
1.2	VOLLEBEKK RESEARCH FARM	3
1.3	REQUIREMENTS	3
1.4	THE SCOPE OF THE THESIS	5
<b>2</b>	<b>METHODOLOGY</b>	<b>6</b>
2.1	TERMINOLOGY	6
2.1.1	<i>Abbreviations</i>	6
2.1.2	<i>Equations</i>	6
2.2	PUGH'S METHOD	7
2.3	SOFTWARE	8
<b>3</b>	<b>THEORY</b>	<b>9</b>
3.1	PHENOTYPING	9
3.2	MATERIALS	9
3.2.1	<i>Metals</i>	12
3.2.2	<i>Composites</i>	13
3.3	PRODUCTION METHODS	13
3.3.1	<i>Composite</i>	13
3.3.2	<i>Metal</i>	14
3.3.3	<i>Plasma Cutting</i>	14
3.4	ASSEMBLY TECHNIQUES	14
3.4.1	<i>Adhesive</i>	14
3.4.2	<i>Bolts and Rivets</i>	15
3.5	MOTORS	15
3.5.1	<i>Electric Motor</i>	16
3.6	TRANSMISSION	18
3.6.1	<i>Gears</i>	18
3.6.2	<i>IP Standard</i>	19
3.6.3	<i>Belts</i>	20
<b>4</b>	<b>POWER REQUIREMENTS</b>	<b>22</b>
4.1	GRADIENT RESISTANCE	22
4.2	DRAG FORCE	23
4.3	ACCELERATION	23
4.4	ROLLING RESISTANCE	24
4.5	FRICTION RESISTANCE	25
4.6	TORA POWER REQUIREMENTS	25
<b>5</b>	<b>COMPONENT SELECTION</b>	<b>27</b>
5.1	MOTOR	27
5.2	TRANSMISSION	27
5.2.1	<i>IP Standard</i>	28
5.2.2	<i>Belt and Pulley</i>	28
5.3	SELECTED COMPONENTS	29
5.3.1	<i>Motor – 3Men BL840</i>	29
5.3.2	<i>Motor controller – SBL 1360</i>	30
5.3.3	<i>Planetary gear – Apex Dynamics AL110</i>	31
5.3.4	<i>Timing belt</i>	32
5.3.5	<i>Wheels</i>	33
5.4	VERIFICATION OF DRIVETRAIN TORQUE CAPACITY	35

<b>6</b>	<b>DIMENSIONING OF THE TORA MODULE .....</b>	<b>39</b>
<b>7</b>	<b>WHEEL MODULE MODIFICATIONS.....</b>	<b>43</b>
<b>8</b>	<b>DESIGN OF COVERS .....</b>	<b>45</b>
8.1	MATERIALS .....	45
8.2	ASSEMBLY TECHNIQUE .....	45
8.3	WHEEL COVERS .....	48
8.3.1	<i>Round</i> .....	48
8.3.2	<i>Triangle</i> .....	49
8.3.3	<i>Pipes</i> .....	50
8.4	COVER ANGLE.....	51
8.5	COVER SELECTION .....	52
8.5.1	<i>Shape</i> .....	52
8.5.2	<i>Cover Angle</i> .....	53
<b>9</b>	<b>DISCUSSION .....</b>	<b>55</b>
9.1	STEERING .....	55
9.2	TORA MODULE .....	56
9.3	WHEEL COVERS .....	56
<b>10</b>	<b>CONCLUSION.....</b>	<b>58</b>
<b>11</b>	<b>BIBLIOGRAPHY .....</b>	<b>59</b>
<b>12</b>	<b>APPENDIX .....</b>	<b>62</b>



# 1 INTRODUCTION

## 1.1 THE THORVALD PROJECT

The Thorvald project has been ongoing for several years now. Pål Johan From with a team of four master students started the project in 2014, and they designed and built the agricultural robot Thorvald I, Figure 1-1. Their goal was to build a light weighted robot to replace big and heavy tractors. Soil compaction is a big problem in farming industry. To keep up with the increase in humans and demand for food, bigger tractors and bigger equipment have been built. Now it has gone too far. Tractors are so big and heavy, and soil compaction is a bigger problem than before. Soil compaction reduces the capacity of plant growth. Many resources are used to fix this problem. Every year, the farmer must plow his fields to make it less compact. By avoiding compaction with a light robot, we reduce the resources needed.

To navigate itself, the robot is equipped with sensors and navigation systems. It should be able to work 24 hours a day, seven days a week, with minimal supervision. The idea is to have several robots that can work on their own, both day and night, instead of a big tractor managed by a driver.



**Figure 1-1: The agricultural robot Thorvald I**

In 2015, the focus was on making equipment for Thorvald. There were several master students, and they were working on making equipment for weed removal, seeding, etc.

Two years after Thorvald I was built a new team of master students designed and built Thorvald II, which is a modified version of Thorvald I. Thorvald I is modular in some ways, and the goal with Thorvald II was to take modularity even further, Figure 1-2. They wanted to have a resizable frame and be able to use different wheel modules. Different types of wheel modules; four-wheel drive and steering, two-wheel drive with differential steering etc. can be chosen depending on its application. Customers can customize it for specific applications. They also wanted to have as many identical components as possible to make production more efficient.



**Figure 1-2: Thorvald II modularity examples. Image: Marius Austad**

In Figure 1-3, Thorvald II is made narrower to fit between the rows in a strawberry tunnel. In early March 2017, a group of students went to the SIMA conference in Paris. There were a lot of interest in Thorvald, and people saw great potential in using the taller module, the second robot from the right-hand side in Figure 1-2. They said that this robot might be of great use in wine yards in France. By those means, only the imagination can stop this progress.



**Figure 1-3: Thorvald II in a strawberry tunnel. Image: Benjamin Alexander Ward**

When this semester is over it will be designed two modified versions of Thorvald II, as well as a carrier for strawberry trays. The following modified versions will be built using modules from the Thorvald II platform:

- Vollebekk, a research farm in Ås, has ordered a robot for phenotyping
- Kristian Guren, a cucumber farmer in Rygge, has ordered a smaller robot to drive inside a cucumber greenhouse

This year's team of master students consists of me (Kristine Skattum), Rémy Nazir Bård Zakaria, Erling Bjurbeck, Eirik Wormdahl, Eirik Solberg and Eivind Bleken. I am going to make Tora, the phenotyping robot, and Remy is going to make a smaller robot for the cucumber greenhouse. Erling is making a carrier/transporter device for carrying strawberries. Eirik W is making a security system for Thorvald. Eivind is analyzing pictures from Vollebekk's phenotyping project last year. Eirik S is working on machine learning.



## 1.2 VOLLEBEKK RESEARCH FARM

Vollebekk is a research farm in Ås. They have different types of research, including phenotyping, which is the observation of grain health. A robot to be used for phenotyping is ordered. As can be seen in Figure 1-4, Thorvald is not tall enough to drive over fully grown plants, and some modifications are therefore necessary. In Ås there is a stereotype of the local student, they are called Thorvald and Tora. For that reason, the tall module will be called Tora.



**Figure 1-4: Thorvald I in the phenotyping field at Vollebekk research farm. Image: NMBU**

In Vollebekk's new project, drones and a modified version of the NMBU-developed agricultural robot Thorvald will collect data with hyperspectral cameras and image analysis to automate measurements made in experimental fields. By taking a series of pictures next to each other, a three-dimensional model can be built and the field can be reproduced in a virtual way. The robot Thorvald drives over the plants and takes close-ups that are linked to three-dimensional image models from drones. This makes it easy to know the field positions of the close-ups.

For more information about the project, see reference [1].

## 1.3 REQUIREMENTS

When designing this robot, both requirements from the Thorvald project and Vollebekk research farm must be fulfilled.

Tora is part of a big project, which sets some limitations. Compared to similar projects, the main difference with Thorvald is its modularity. Having this in mind when designing and selecting components is therefore of great importance. These are the requirements from the Thorvald project:

- Keep as many of the standard Thorvald modules and components as possible to retain the modularity
- Low weight

The robot will drive in a phenotyping field at Vollebekk research farm, and to avoid causing any damages on plants, some requirements are listed:

- Narrower robot, 150 mm wheel, gear and wheel module width
- Taller robot, about 170 cm from ground to top
- Covers 15 cm above ground with a 30° angle, see Figure 1-5, separating grains in front of the wheels
- Enough power to handle flat fields

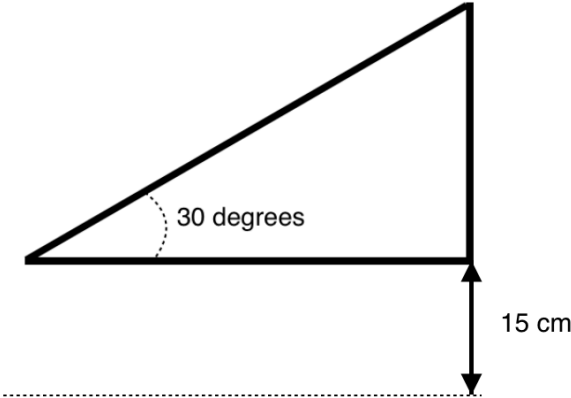


Figure 1-5: Illustration showing height above ground and angle requirement for the wheel cover

Table 1-1 shows an overview of all the requirements with a number for importance. The scale ranges from 1-5, where 5 is the one of highest importance.

Table 1-1: Overview of requirements with importance

Modularity	Concept	5
Power	Handle flat fields	5
Narrower and taller	Drive in the research field without causing damage	5
Low weight	Concept	2
Covers 15 cm above ground	Should be able to avoid rocks	4
Cover angle 30°	Concept known to work	3
Cost	Affordable	2

## 1.4 THE SCOPE OF THE THESIS

The purpose of this thesis is to design and build a modified robot, Tora, capable of driving in grain fields without causing any damages on grains, and determine components best suited for this application. Having all the requirements stated in mind is of great importance when making decisions. To fulfill the requirements set by Vollebekk research farm in addition to keeping the modularity of Thorvald is a big challenge. Vollebekk have practical knowledge of designs that are functional on big and heavy tractors, but not small machines like a robot. A robot will be used, and the thesis will therefore face challenges that makes it hard to satisfy all the demands. Some requirements will most likely be left out, and good explanations must state the reasons for the absences with new solutions following.

The structural foundation of Thorvald II will form the base of Tora. However, the focus in this thesis will be to design a grain field and phenotyping research robot. Today, this is done manually, low throughput. Through usage of Thorvald's robot technology, this can be done more efficient, high throughput. Flat fields are the only application areas for this specific robot, and two-wheel drive with caster wheels and differential steering was therefore chosen prior to this thesis. Through discussion, different steering solutions will be discussed to find out if the right decision was made.

Components will be selected based on existing software and communication protocol so that the robot can be controlled with high precision.

A robot is to be designed and built in four months, time is therefore a limiting factor that must be considered when choosing components. Fast installation solutions are required if the platform is to be completed in time.

Even though keeping the robot weight and price at a minimum is a goal, this cannot come at the cost of low quality. Use in the field will be this robot's main purpose, and therefore handling conditions associated with field operations is of great importance.

Unfortunately, the deadline of this thesis is May 15, and the robot will most likely not be completed within this short timeframe. The goal is to get the designed parts ready for the defending, and the entire robot finished before the grains are too tall for Thorvald II.

**Goal:** Design a modified version of Thorvald to fit necessary requirements to drive in a phenotyping field, and start the production of the robot.

## 2 METHODOLOGY

### 2.1 TERMINOLOGY

#### 2.1.1 ABBREVIATIONS

AC	Alternate Current	DC	Direct Current
BDC	Brushed DC motor	BLDC	Brushless DC motor
FCC	Face-Centered Cubic	BCC	Body-Centered Cubic
HCP	Hexagonal Close-Packed	CNC	Computer Numeric Control
SIMA	Salon International du Machinisme Agricole	NMBU	Norwegian University of Life Sciences
W	Watt	MW	Mega Watt
N	Newton	RPM	Revolutions Per Minute
BL	Brushless	CAN	Control Area Network
MPa	Mega Pascal	A	Ampere
CAD	Computer Aided Design	FEM	Finite Element Method
3D	Three-Dimensional		

#### 2.1.2 EQUATIONS

Von Miseses

$$\sigma_{eq} = \sqrt{\sigma_x^2 + \sigma_y^2 - \sigma_x\sigma_y + 3\tau_{xy}^2} \quad (3-1)$$

Specific Strength

$$\text{Specific Strength} = \frac{\text{Tensile Strength}}{\text{Specific Weight}} \quad (3-2)$$

Gradient Resistance

$$F_g = mg * \sin(\alpha) \quad (4-1)$$

Drag Force

$$F_D = \frac{1}{2} C_D A \rho v^2 \quad (4-2)$$

Acceleration Torque	$M_A = \alpha_A \left( I_A + \frac{I_B}{(i_{A \rightarrow B})^2 \eta_{A-B}} + \frac{I_C + \frac{m}{n_w} r_w^2}{(i_{A \rightarrow C})^2 \eta_{B-C}} \right)$	(4-3)
Rolling Resistance	$F_r = C_{rr}$	(4-4)
Friction Resistance	$F_f = \mu_k N$	(4-5)
Power	$P = F \times v$	(4-6)
Moment of Inertia of a Cylinder	$I_{cylinder} = \frac{1}{2} m_{cylinder} r_{cylinder}^2$	(5-1)
Moment of Inertia of a Thin Disc	$I_{cylinder} = \frac{m_{thindisc} r_{thindisc}^2}{2}$	(5-2)

## 2.2 PUGH'S METHOD

Pugh's method [2], also called decision-matrix-method, will be used to compare different components and designs. Different advantages and drawbacks are included in this matrix, where criteria of importance are listed.

**Table 2-1: Model of a decision matrix with 4 alternatives, 4 criteria, weighting, score(X), weighted score(Y), and weighted sum(Z)**

	Weighting	Alternative 1		Alternative 2		Alternative 3		Alternative 4	
Criteria 1	40 %	X	Y	X	Y	X	Y	X	Y
Criteria 2	30 %	X	Y	X	Y	X	Y	X	Y
Criteria 3	10 %	X	Y	X	Y	X	Y	X	Y
Criteria 4	20 %	X	Y	X	Y	X	Y	X	Y
Criteria Sum	100 %	<b>Z</b>		<b>Z</b>		<b>Z</b>		<b>Z</b>	

Table 2-1 shows an example of how a decision matrix may look based on Pugh's method. In this example, the alternatives will be judged based on 4 criteria with different weightings based on their importance.

## 2.3 SOFTWARE

- **SolidWorks 2016/2017**
  - Computer Aided Design (CAD) program used for 3D-modelling.
  - Photoview 360 is used for rendering of pictures of the SolidWorks model.
- **ANSYS Workbench 17.2**
  - Finite Element Method (FEM) used for stress analysis.
- **Microsoft Excel**
  - Used for simple calculations and graphs.
- **Microsoft Word**
  - Used for report writing
- **Pages**
  - Program used to edit and modify pictures.



(a)



(b)



(c)



(d)



(e)

Figure 2-1: Software logos. (a) SolidWorks, (b) Pages, (c) ANSYS, (d) Microsoft Word, (e) Microsoft Excel

### 3 THEORY

This master's thesis is part of a big project, and the theory part is therefore based on previous work. Many of the parts being used in this thesis were selected several years ago by master students, previous master's thesis are therefore used as ground stones in this chapter; Lars Grimstad [3], Fredrik Blomberg [4], Marius Austad [5], and Øystein Tårnes Sund [6].

#### 3.1 PHENOTYPING

Phenotyping is defined as the observation of grain health. This is done in special research fields, Figure 3-1, where grains are divided into squares. The goal of this research is to create new plant varieties, which is necessary to increase crop yields, and to improve adaptations to climate changes.



Figure 3-1: Phenotyping field [7]

To create a virtual field, researchers use multispectral and hyperspectral cameras to capture images. The advanced images allow researchers to access information that eyes do not see. A hyperspectral camera can take pictures showing both the visible and the invisible light. Light reflection from chlorophyll and greenery of the foliage reveal the plant's state. Information contained in the infrared area tells about the physiological status of the plant, for example if the plants are stressed or sick.

For more information, see reference [1].

#### 3.2 MATERIALS

Solid materials are grouped into three categories; metals, ceramics and polymers. These categories are made primarily based on atomic structure and chemical makeup, and most materials fall into one of these groups. If different materials are combined, new materials with entirely different characteristics than the materials by themselves are made. To achieve desired properties, there is also possible to heat treat some materials. There are many types of materials to choose from, but it should not be too difficult to choose the right one for a specific project.

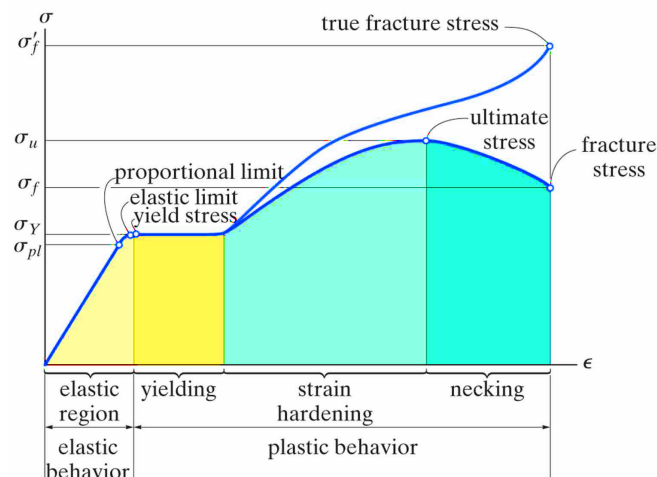
**Modulus of Elasticity (Young's modulus)** represents the constant of proportionality in Hooke's law. Thomas Young published an account of it in 1807, which is why the name is Young's modulus. The modulus of elasticity represents the slope in a stress-strain diagram, Figure 3-2, and indicates the stiffness of a material. Very stiff materials have high values, whereas spongy materials have low values. For metals, the value ranges between 45 GPa and 407 GPa.

**Poisson's number** is the relationship between a material's cross-sectional area and elongation. The cross-sectional area will either decrease or increase as the material stretches or compresses. The value for aluminum and steel is usually around 0.3.

**Shear modulus** is a materials ability to resist shear forces. It represents the relationship between Young's modulus and Poisson's number.

**Yield strength** is stress that causes yielding. It occurs when stress increases slightly above the elastic limit, and this point is called yield stress. Yielding results in a breakdown of materials and a permanent deformation, called plastic deformation. Yield stress is shown in Figure 3-2.

**Tensile strength** is the ultimate stress, or maximum stress a material can handle. After yielding, an increase in load results in a curve that rises continuously, but becomes flatter, until it reaches ultimate stress, see Figure 3-2. The cross-sectional area decreases uniformly over the length as the stress moves towards ultimate stress. After reaching ultimate stress, the cross-sectional area will begin to decrease in a localized region. This tends to result in the forming of a constriction or neck. The curve in the stress-strain diagram will then tend to curve downwards until the material breaks at fracture stress, Figure 3-2.



Conventional and true stress-strain diagrams for ductile material (steel) (not to scale)

Figure 3-2: Stress-strain diagram [8]

Yield strength is used as the maximum stress for design purposes to cite the strength of a material. If tensile strength is used for this purpose, the design will be useless before it reaches maximum allowed stress. This is usually because the design will experience a large plastic deformation before it reaches this point.



**Equivalent stress (Von Mises hypothesis)** is a theory that has the closest comparison with reality when considering ductile materials like construction steel, aluminum and copper [9]. It states that the shape changes made by shear stress must be taken into account when considering multi-axis loads. This stress, equivalent stress, can then be compared to yield- or tensile strength. As the name states, Von Mises hypothesis, this stress is hypothetical and in one direction.

Von Mises hypothesis can be expressed by an equation;

$$\sigma_{eq} = \sqrt{\sigma_x^2 + \sigma_y^2 - \sigma_x\sigma_y + 3\tau_{xy}^2} \tag{3-1}$$

Where

$\sigma_{eq}$  is the equivalent stress

$\sigma_x$  is the x-component stress

$\sigma_y$  is the y-component stress

$\tau_{xy}$  is the shear stress

For more information on material properties, see [10].

Material strength is usually described by the Specific Strength. The value is the Tensile Strength to Specific Weight ratio, and is shown in equation (3-2).

$$\text{Specific Strength} = \frac{\text{Tensile Strength}}{\text{Specific Weight}} \tag{3-2}$$

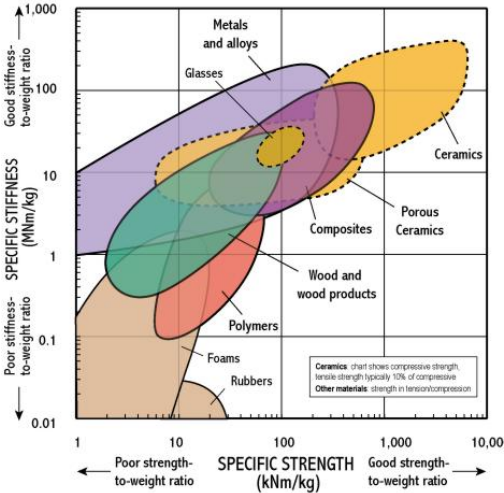


Figure 3-3: Material properties. Specific Stiffness vs. Specific Strength [11]

This value is important when designing high-efficient, low-weight systems, such as a robot where energy consumption is a priority. Figure 3-3 shows a comparison of different material's Specific Strength and Specific Stiffness.

### 3.2.1 METALS

Metals are composed of one or more metallic elements, such as iron, aluminum and copper, and often also nonmetallic elements, such as carbon, nitrogen and oxygen, in relatively small amounts. In metals and their alloys, atoms are arranged in an orderly manner and are relatively dense in comparison to the ceramics and polymers. Its mechanical characteristics make these materials relatively stiff and strong, but still ductile and resistant to fracture, which make them widely used materials in structural applications.

*“A crystalline material is one in which the atoms are situated in a repeating or periodic array over large atomic distances”* [12], and solids may be classified according to the regularity with which atoms and ions are arranged with respect to one another. All metals, many ceramics and some polymers form crystalline structures under normal conditions. Structure are often subdivided into small repeat entities called unit cells when describing crystal structures. For most crystal structures, unit cells are parallelepipeds or prisms that represents the symmetry of the crystal structure.

For the most common metals, there are three simple crystal structures; face-centered cubic, body-centered cubic and hexagonal close-packed. The *face-centered cubic (FCC)* crystal structure has atoms located at each corner and the centers of all the cube faces, see Figure 3-4 (a). Some examples of metals with this structure are copper, aluminum, silver and gold, which are relatively soft metals.

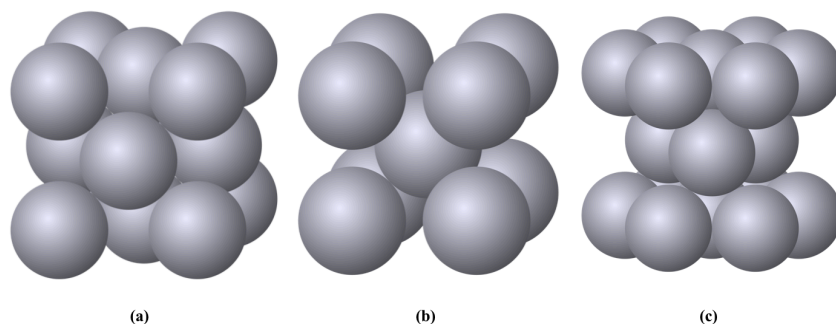


**Figure 3-4: Metallic Crystal Structures, (a) The face-centered cubic, (b) The body-centered cubic, and (c) The hexagonal close-packed [13]**

Another structure which also has a cubic unit cell is the *body-centered cubic (BCC)* crystal structure, see Figure 3-4 (b). The atoms in this crystal structure are located at all eight corners and a single atom in the cube center. Examples of metals with this structure is chromium, iron and tungsten.

The *hexagonal close-packed (HCP)* crystal structure is the final common metallic crystal structure, and has a hexagonal unit cell. The top and bottom faces of the unit cell have six atoms that form regular hexagons and surround a single atom in center. Between top and bottom plane there is a third plane with three additional atoms, see Figure 3-4 (c). Some HCP-metal examples are cadmium, magnesium, titanium and zinc.

### 3.2.2 COMPOSITES

Composites are composed of two or more individual materials from metals, ceramics and polymers [12]. The goal is to achieve a combination of properties that is not displayed by any single material and include the best characteristics from each of the component materials.

Fiberglass is one of the most common composites, where small glass fibers are embedded within a polymeric material. Fiberglass is very stiff, strong and flexible, this is because glass fibers are relatively strong and stiff, and polymers are more flexible.

Carbon fiber-reinforced polymer(CFRP) composite is another important material where carbon fibers are embedded within a polymer. These materials are stiffer and stronger, but more expensive than fiberglass.

## 3.3 PRODUCTION METHODS

The methods of production change with the change in materials, as different materials behave differently. The scale of production is the first factor that must be evaluated before choosing a production method. Materials are chosen based on what kind of production method is being used, or vice versa.

In this chapter, common production methods will be presented with their corresponding materials.

### 3.3.1 COMPOSITE

**Open Molding** is “*a low cost, common process for making fiberglass composite products*” according to Composite World [14]. Further they explain how this involves a one-sided composite mold that is being used repeatedly. The composite mold is made first by making a positive plug of wood. The plug is further painted with a gel coat so that it is easy to remove after curing. This method makes it easy to produce a mold without using heavy machinery. This method becomes more expensive as the production grows, which makes it better suited for small production.

### 3.3.2 METAL

This chapter will focus on production methods using sheet metal. Only sheet metal will be used to keep the robot's weight at minimum.

**Bending** is the straining of material, usually flat sheets, by moving it around an axis that lies in the neutral plane. Within the plastic range, metal flow takes place, and bent parts retain a permanent shape after the applied stress is removed. This gives compression on the inside of the bend, and tension on the outside [15].

### 3.3.3 PLASMA CUTTING

Plasma is a state of matter which is created by heating ionized gas. According to Ramakrishnan, "*The plasma cutting process employs a plasma torch with a very narrow bore to produce a transferred arc to the workpiece*" [16]. Plasma cutters are very useful to cut sheet metal plates in curved or angled shapes, this is because plasma cutters produce a very hot and localized jet to cut with. Plasma cutting machines can be mounted on a CNC machine, so that the entire process can be controlled and optimized by a computer which makes clean and sharp cuts. Parts that require no finishing operations can be obtained by using a combination of CNC technology and a smaller nozzle for a thinner plasma arc [17].

## 3.4 ASSEMBLY TECHNIQUES

### 3.4.1 ADHESIVE

To bond two solid materials(adherends) together, an adhesive can be used. There are many materials that can be used as adherends; metals, ceramics, composites, polymers etc. are some examples. This technique is used in many applications, including construction, furniture, automotive, aircrafts etc. [18].

There are many types of adhesives, and choosing the right kind depends on the application, such as which materials that are being combined, if the bonding is going to be temporary or permanent, what temperatures the product will be exposed to, and processing conditions.

Adhesive bonding has a great amount of advantages. According to Irving Skeist, "*Thin films, fibers and small particles, that could not be combined so well, or at all, by other techniques, are readily bonded with adhesives*" [18]. Achieving lighter and stronger assemblies than with mechanical fastening is possible because the stresses are distributed over wider areas. With adhesives, dissimilar materials can be joined and compared to other techniques, it is faster and cheaper.

Temperature changes is one challenge when using adhesives. At relatively low temperatures, polymers can maintain their mechanical toughness. As temperature increases, strength decreases rapidly. At temperatures of 300°C, only a few polymers can be used continuously.

### 3.4.2 BOLTS AND RIVETS

Rivets was for many years the only method of connecting structural steel. But due to the ease and economy of welding and high-strength bolts, the use of rivets has declined in the recent years. Rivets are usually made from a soft steel that does not become brittle when heated and hammered with a riveting gun [19]. The rivet is placed in the holes of joining materials, and driven flat on one side, as seen in Figure 3-5.

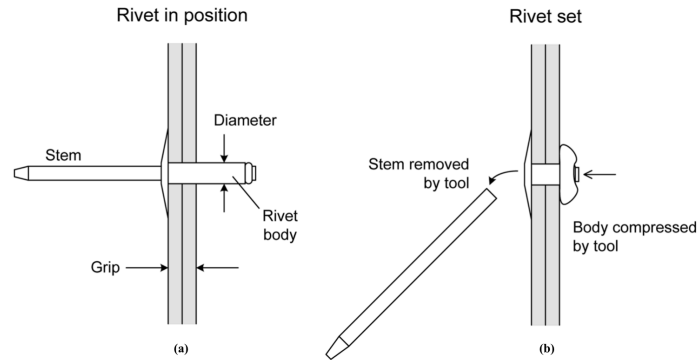


Figure 3-5: Rivet (a) before driving, and (b) after driving [20]

If a rapid field-erection process method is needed to join steel structures, bolting is a good solution. It has an advantage, because it requires less skilled labor than riveting and welding [19]. Another advantage is that the connection is not permanent. It can easily be removed and used almost everywhere. Bolting has become the leading method in connecting structural steel in the field.

### 3.5 MOTORS

The traction between wheel and surface, and the maximum torque provided by the on-board power plant and transmission are two limiting factors of a vehicles performance. The potential of the vehicle will be determined by the smaller of these two factors.

A large amount of torque at low speeds are desired in a power plant when the robot is accelerating or grade climbing, and, over a wide speed range, maintaining a constant power output, see Figure 3-6.

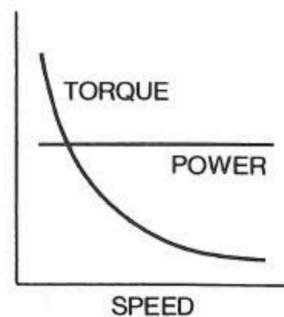


Figure 3-6: Ideal vehicle performance characteristics [21]

Motor is defined as “any of various power units that develop energy or impart motion, such as a rotating machine that transforms electrical energy into mechanical energy”, and transmission is defined as “an assembly of parts including the speed-changing gears and the propeller shaft by which the power is transmitted from an engine to a live axle” by Merriam-Webster on-line dictionary [22].

If speed is exchanged for torque, or the other way around, the word transmission is used. A transmission is used to transmit the power from high speed, low torque motor shaft, to a low speed, high torque output shaft, when combustion engines or electric motors are being used. This is because these types of motors generally operate at higher speeds than what is desired for most applications.

In the following, electric motors will be discussed because this will value Thorvald’s concept of modularity.

### 3.5.1 ELECTRIC MOTOR

Electric motors convert electric energy from an alternate current (AC) or a direct current (DC) source to mechanical energy at a rotating shaft. Electric motors has ratings from 0.2W [23] to 100 MW and higher [24]. These motors can be found in anything from watches and toys to cars, trains, ships and factories. There are many different types, but the main ones are induction motors and its derivatives which are equipped with a commutator, Schrage motors, synchronous motors, and DC motors [25]. DC motors are very suitable for mobile applications because they can run on batteries. Thorvald is already using DC motors, the following information will therefore only include DC motors.

For more information on other types of electric motors, see [25].

A DC motor has two parts; a rotor (the rotating part) and a stator (the stationary part), see Figure 3-7. There are two types of DC motors; Brushed DC motor (BDC), Figure 3-7, and Brushless DC motor (BLDC), Figure 3-8. The simplest edition of a DC motor is BDC, and because of its early development it is still very popular. BDC motors are in general affordable, and do not need complex drive electronics. The lifetime is limited because there is direct contact between brushes and commutator. They will wear out and need maintenance. This motor is also significantly larger than brushless motors [26].

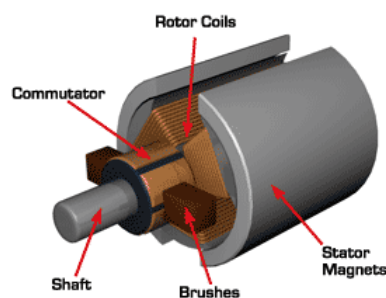


Figure 3-7: Brushed DC motor [27]

## Brushless DC (BLDC) motor

According to Yedamale, “*Brushless Direct Current (BLDC) motors are one of the motor types rapidly gaining popularity*” [28]. They are used in industries like automotive, aerospace, medical, industrial automation etc. As the name implies, it does not have brushes for commutation; they are instead electronically commutated.

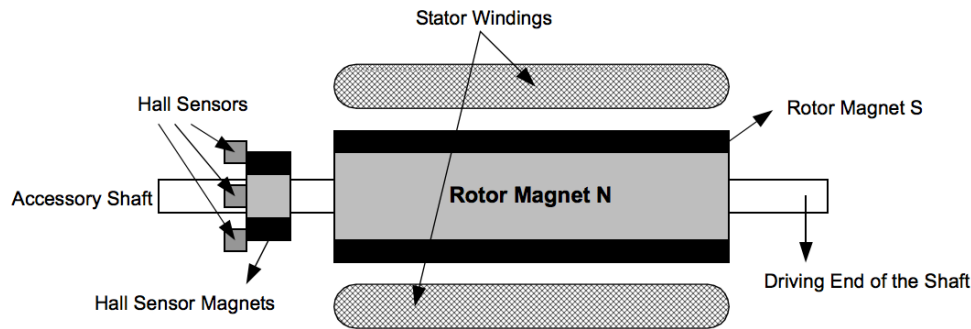


Figure 3-8: Cross section of a BLDC motor [28]

1-, 2- and 3 phases are available for the BLDC motor; 1-phase is used for low-power applications, 2-phase for medium-power applications, and 3-phase for high-power applications. 3-phase is better suited for driving and steering. For this reason, only 3-phase will be taken into consideration.

“*Most BLDC motors have three stator windings connected in star fashion*”, Yedamale [28]. Each of them are distributed over the stator periphery to form an even number of poles. The stator windings should be energized in a sequence to rotate the BLDC motor. To understand which winding will be energized following the energizing sequence, it is important to know the rotor position. By embedding Hall effect sensors into the stator, the position is sensed. BLDC motors usually have three of these sensors on the non-driving end of the motor, see Figure 3-8. Hall sensors give a high or low signal, indicating N or S pole, whenever the rotor magnetic poles pass. The exact sequence of communication can be determined based on the combination of these three sensor signals.

BLDC motors have many advantages over brushed DC motors and induction motors [28]:

- Better speed versus torque characteristics
- High dynamic response
- High efficiency
- Long operating life
- Noiseless operation
- Higher speed ranges

In applications where space and weight are critical factors, BLDC motors are leading. This is because the ratio torque delivered to the size of the motor is higher.

## 3.6 TRANSMISSION

A device is mounted between the power source and the specific application to combine the two components together, this device is called transmission. With constant- or variable ratio of the output to input speed, most transmissions functions as rotary speed changers [29]. The robot will operate within a low range of speeds, this thesis will therefore only focus on transmissions with constant ratio.

### 3.6.1 GEARS

Gears are meshed toothed wheels with no slip, and are used to transmit power or motion between two shafts. The smaller wheel is called “pinion” and the larger wheel is called “gear” in a pair of wheels. If the power input is at the pinion, it results in a decrease in output speed and an increase in torque. If the power input is at the gear, the result is opposite, with an increase in output speed and a decrease in torque.

#### **Spur Gears**

According to Gibbs Gears, “*Spur gears are the most common type of gears. They have straight teeth, and are mounted on parallel shafts*” [30]. Figure 3-9 shows a spur gear. They are popular gears because they are simple, and easy to manufacture and maintain. The problems with spur gears are that the design creates a lot of stress on the gear teeth. The design also makes the gear quite noisy, when used at high speeds it makes a sound every time the gear teeth collide with each other. For this reason, spur gears are known as slow speed gears [31].

#### **Helical Gears**

The teeth mesh gradually and the full width of any one tooth is never completely engaged in helical gearing, shown in Figure 3-9. This adjustment reduces noise and stresses on the gear teeth associated with spur gears. These gears are also called spiral or skew helical gears [31].

#### **Herringbone Gears**

Herringbone gear is also called double helical gear because of its shape, see Figure 3-9. According to Hewitt & Topham, “*Double helical gears give the same advantage and smoothness as single helical gears, but with the added value of a much greater strength in the contact of the teeth and no sideways force or end load on the mounting shafts*” [31]. Herringbone gears have a complicated shape, which makes them more difficult to produce and hence more expensive than other gears.

#### **Planetary Gears**

Planetary or epicyclic gearing is a transmission system consisting of one or more outer gears, or planet gears, revolving around a central gear, or sun gear [30]. Figure 3-9 shows the layout of a planetary gear with three planet gears. These gears can transfer high torques with high efficiency. This is because the loads are distributed over multiple planet gears. Compact design is one of the gear’s advantages.





(a)



(b)



(c)



(d)

**Figure 3-9: Different gear types. (a) Spur gear, (b) Helical gear, (c) Herringbone gear, (d) Planetary gear [30]**

For more information on gears, see reference [32].

### 3.6.2 IP STANDARD

IP codes classifies the rate of closure/protection against dust and water. The gears used for Thorvald today is IP67. The first digit represents protection against solid particles, Table 3-1, and the second digit protection against liquid ingress, Table 3-2 [33].

**Table 3-1: Solid particle protection**

Digit	Effective against	Description
0	-	No protection
1	>50 mm	Any large surface of body
2	>12.5 mm	Fingers or similar objects
3	>2.5 mm	Tools or thick wires
4	>1 mm	Most wires, slender screws or large ants
5	Dust protected	Ingress of dust is not entirely prevented
6	Dust tight	No ingress of dust

**Table 3-2: Liquid ingress protection**

Digit	Effective against	Description
0	None	-
1	Dripping water	Dripping water shall have no harmful effect
2	Dripping water when tilted 15°	Vertically dripping water shall have no harmful effect
3	Spraying water	Water falling as a spray at any angle up to 60° from vertical
4	Splashing of water	Water splashing against the enclosure from any direction
5	Water jets	Water projected by a nozzle (6.3 mm) against enclosure
6	Powerful water jets	Water projected in powerful jets (12.5 mm) against enclosure
7	Immersion, up to 1m depth	Ingress of water in harmful quantity shall not pass through the enclosure
8	Immersion, 1m or more depth	Suitable for continuous immersion in water

### 3.6.3 BELTS

Belts are used to transfer power from one component to another by using rotating pulleys. If pulleys with different sizes are applied, there will be a ratio in speed of the two components. For applications where layout flexibility is needed, belt drives are very useful. Components can be placed on preferable locations and still achieve the same efficiency [34].

There are three main types of belt drives; flat belts, v-belts and circular belts, see Figure 3-10. Flat belts are an old design with moderate efficiency, the same can be said about circular belts, which limits their applications to low power devices.

#### V-belts

According to the authors of “Engineering Principles of Agricultural Machines”, “*V-belts are employed extensively in agricultural machinery applications in which it is not necessary to maintain exact speed ratios*” [35]. V-belts have matching pulleys, which fits perfectly. They can operate at speeds up to about 33 m/s, although agricultural machines rarely exceed 15 m/s. The main drawback of such belts is the tendency for the belt to slip over time.

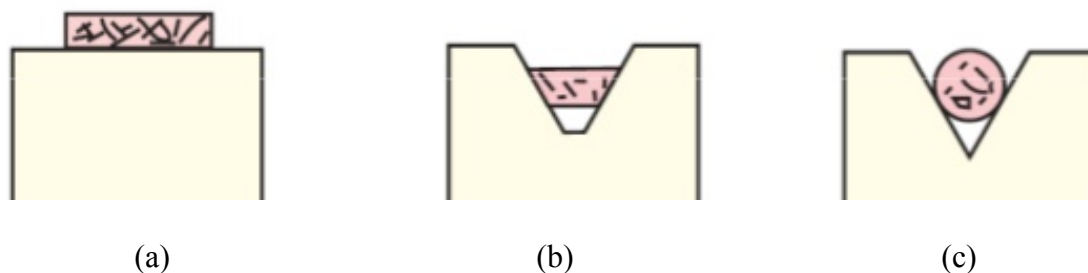


**Figure 3-10: (a) Flat belt, (b) V-belt and (c) Circular belt [36]**

### Timing belts

Another alternative is timing belts; belts with teeth. With timing belts, there are no relative motion between the two elements, and the belt has no slip. This means that they have synchronous drive (or positive drive) [37]. Teeth make sure that the load is spread out to all teeth in contact with the pulley. Some tooth profiles are shown in Figure 3-11. Trapezoidal tooth profiles are most common. A drawback is issues with deformation which increases wear causing noise [34].

According to Paul E. Sandin, “Timing belts can be used at very low rpm, high torque, and at power levels up to 250 horsepower” [37]. They can be used in wet conditions, but have a slightly higher price than the alternatives.

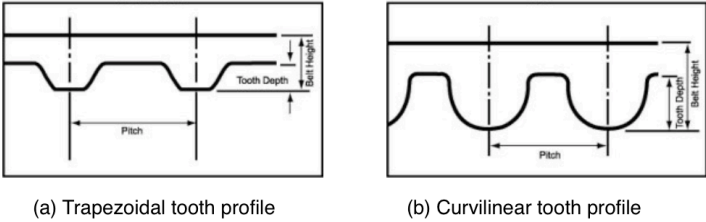


Figure 3-11: Timing belts [38]

## 4 POWER REQUIREMENTS

Estimating required power for a robot is difficult, since there are not many agricultural robots on the market today. Thorvald II has been successful, it can withstand the loads it is dimensioned for. For this reason, the same calculation method for power requirements will be used for Tora.

Tora will have a two-wheel drive, with differential steering, and weighs about 200 kg when fully equipped. The robot will drive in a research field, with no steep hills or heavy terrain. For this reason, Tora does not need as much power as Thorvald II. This chapter will cover propulsion on the two front wheels.

### 4.1 GRADIENT RESISTANCE

Tora will not climb as steep hills as Thorvald II, but there will still be uneven ground. To be safe gradient resistance will be considered.

When the robot is driving in hills, the weight of the robot can be divided into two force vectors; one parallel and one perpendicular to the ground. The one pulling the robot down hills is the one parallel to the ground, gradient resistance. This force is calculated by multiplying the weight of the robot with sine of the hill angle, see equation (4-1). The robot's power must exceed the gradient resistance to climb hills.

$$F_g = m.g * \sin (\alpha) \quad (4-1)$$

Where

$F_g$  is the gradient resistance

$m$  is the vehicle's mass

$g$  is the gravitational constant with a value of  $9.81 \text{ m/s}^2$

$\alpha$  is the hill angle

The forces applied can be seen in Figure 4-1.

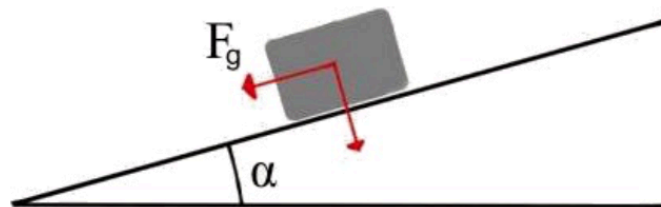


Figure 4-1: Gradient resistance

## 4.2 DRAG FORCE

Air resistance, or drag force, is generated when air flows over the body of a driving vehicle. As seen in equation (4-2), the magnitude of the forces increases with the square of the relative velocity between air and vehicle. This friction force can therefore have a great negative impact on efficiency for a moving vehicle at high speeds. Drag forces can reduce efficiency with more than the vehicle's speed at low speeds. For this reason, winds should be considered for slow vehicles, where wind speeds might be greater than the speed of the vehicle.

Vehicles will behave differently when exposed to drag forces. This is because different vehicles have different shapes and sizes. A vehicle's ability to cut through air can be expressed by its drag coefficient. A sports car's shape, for example, is smoother than regular cars to increase the ability to cut through air.

The density of fluids the vehicle must cut through needs to be considered. This fluid is normally air, but there might be other fluids in some applications. The area of the vehicle's projection where the fluid impacts, usually the front of the vehicle, must also be considered. The drag force is calculated using equation (4-2).

$$F_D = \frac{1}{2} C_D A \rho v^2 \quad (4-2)$$

Where

$F_D$  is the drag force

$C_D$  is the drag coefficient

$A$  is the area of the vehicle's projection

$\rho$  is the density of the fluid

$v$  is the speed of the fluid relative to the vehicle

## 4.3 ACCELERATION

To accelerate a motor, a torque that is equal to desired angular acceleration multiplied with mass moment of inertia of the motor is needed. For this robot, there will be a powertrain connected to the motor, and the equivalent moment of inertia of the components must therefore be calculated with respect to the motor.

The mass of the vehicle must be considered, because of its great importance in the Thorvald project. The mass of the vehicle is included by first dividing mass by the number of drive wheels, then multiplying this with the square of the wheel radius. This results in a mass moment of inertia representing the mass of the vehicle with respect to the wheel shaft. Furthermore, the equivalent moment of inertia is calculated with respect to the motor shaft and added to those of the other components.

Equation (4-3) calculates a simplified acceleration torque, Figure 4-2, but it should give good enough results.

$$M_A = \alpha_A \left( I_A + \frac{I_B}{(i_{A \rightarrow B})^2 \eta_{A-B}} + \frac{I_C + \frac{m}{n_w} r_w^2}{(i_{A \rightarrow C})^2 \eta_{B-C}^2} \right) \quad (4-3)$$

Where

$M_A$  is the acceleration torque of shaft A

$\alpha_A$  is the angular acceleration of shaft A

$I$  is the moment of inertia of each shaft

$\eta$  is the efficiency of each power transmission stage

$m$  is the mass of the vehicle

$r_w$  is the radius of the drive wheels

$n_w$  is the number of drive wheels

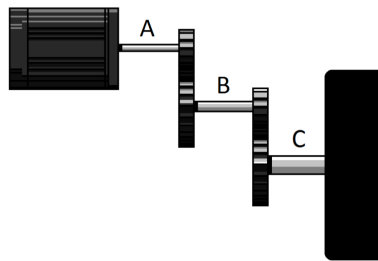


Figure 4-2: Powertrain example

#### 4.4 ROLLING RESISTANCE

There is a force resisting the force of the vehicle when it rolls on surfaces. When a vehicle, for example an agricultural robot, moves through a terrain, both the tires of the vehicle and the ground gets deformed. When pressure is released, some of the energy consumed by the deformation is recovered, but not all of it. This force is called rolling resistance and is calculated by multiplying normal force on the tire from the ground with a resistance coefficient, see equation (4-4). This coefficient depends on tire type and ground surface.

$$F_r = C_{rr} N \quad (4-4)$$

Where

$F_r$  is the rolling resistance force

$C_{rr}$  is the rolling resistance coefficient

$N$  is the normal force. The force perpendicular to the ground acting on the wheel.

## 4.5 FRICTION RESISTANCE

According to R. Nave, “*Frictional resistance to the relative motion of two solid objects is usually proportional to the force which presses the surface together as well as the roughness of the surface*” [39]. The ratio of the frictional resistance force to the normal force which presses surfaces together is the coefficient of friction, and characterizes the friction.

$$F_f = \mu_k N \quad (4-5)$$

Where

$F_f$  is the friction resistance force

$\mu_k$  is the coefficient of kinetic friction

$N$  is the normal force

## 4.6 TORA POWER REQUIREMENTS

The exact power requirements for Tora is difficult to determine. There must be a sufficient torque exerted on the wheel by the motor to overcome rolling, gradient, friction, and air resistance. All of this while the robot is accelerating from zero to working speed in a short amount of time.

### Minimum Power Requirements

The research field at Vollebekk is somewhat uneven, but the robot will not face very steep slopes. Tora should be able to drive everywhere in the research field at any time, thus it should be strong enough to face terrain in the field, even when carrying maximum load.

The following calculations are done with the worst-case scenarios the robot will face;

- Incline: 7°
- Weight: 200 kg
- Wind speed: 5 m/s
- Vehicle speed: 1.5 m/s

With these factors in mind, and knowing the gravitational acceleration, 9.81 m/s<sup>2</sup>, equation (4-1) gives a gradient resistance of 239.1 N.

On a clam day, the slow working robot can neglect drag forces. However, the robot should be able to handle windy days with wind speeds up to 5 m/s. Estimating drag coefficients and area of projection before the robot has been built is difficult. For this reason, some standard values are used for these calculations. The drag coefficient is set to 0.50, which is the value for an off-road vehicle [40], and the area of projection is set to 0.75 m<sup>2</sup>, based on the rough sketch in Figure 4-3. Density of air is 1.293 kg/m<sup>3</sup> (273K) [40]. If the robot is driving at 1.5 m/s against wind, equation (4-2) gives an air resistance of 10.2 N.

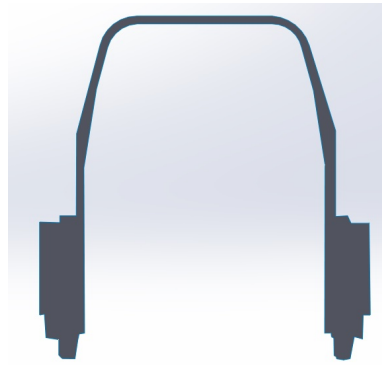


Figure 4-3: Estimated projection of Tora, front view

For rubber tires on dirt, the rolling coefficient can be set to 0.04 according to HP Wizard [41]. For a 200kg robot, equation (4-4) gives a rolling resistance of 78.5 N.

The friction coefficient for rubber tires on dirt can be set to 0.60 according to HP Wizard [41]. The weight of the robot is distributed with about 60 kg on each front wheel and 40 kg on each caster wheel. If one caster wheel, 40kg, for some reason is locked and works as a break, equation (4-5) gives a friction resistance of 235.4 N.

Table 4-1: Summary of the resistance forces

$F_g$ , gradient resistance	239.1 N
$F_D$ , air resistance	10.2 N
$F_r$ , rolling resistance	78.5 N
$F_f$ , friction resistance	235.4 N
<b>Total resistance</b>	<b>563.2 N</b>

The torque needed for acceleration, equation (4-3), will be calculated when the drivetrain is selected. This value will be used as a confirmation after components have been selected.

When the robot is driving with a constant speed, 1.5 m/s, the motor must generate:

$$P = F \times v \quad (4-6)$$

$$P = 563.2 \text{ N} \times 1.5 \text{ m/s}$$

$$P = 844.8 \text{ W}$$

The power transmitted by each wheel must be:

$$\frac{844.8 \text{ W}}{2} = 422.4 \text{ W}$$



## 5 COMPONENT SELECTION

To retain the modularity of Thorvald, the use of previous components will be examined and prioritized.

### 5.1 MOTOR

From previous robots, Thorvald I and Thorvald II, electric motors running on batteries have been used. Based on the value of retaining modularity and good experiences, the decision of keeping the same set up for Tora can be made.

According to the graph in Figure 3-6, a motor with high torque at low speeds is desirable, and electric motors are well suited for this. Even though electric motors offer a high torque, this won't be enough, a transmission is thereby needed. As mentioned in the chapter "Motors", the brushless motors are smaller, more efficient and require less maintenance than the brushed motors. These advantages weigh up for the fact that the brushless motors are more expensive and require a more complex motor controller. With all this in mind, in addition to modularity, a BLDC motor is the best alternative.

### 5.2 TRANSMISSION

The transmission criterions to evaluate are; size, efficiency, price and durability. The components should be compact, have high efficiency, low price and be robust. The component with the highest score is best suited for its application.

Some criterions are more important than others, and is therefore listed with different percentages. The more important, the higher percentage. Since the best possible solution is needed, price will get a low percentage, 10%. All possible solutions have been properly tested, so they should be durable enough, 20%. Size is of great importance for the new robot, 40 %. Efficiency gets the remaining 30 %.

**Table 5-1: Evaluation of different gears**

		Planetary gear		Spur gear		Helical gear		Herringbone gear	
Size	40 %	2	<b>0.8</b>	1	<b>0.4</b>	1	<b>0.4</b>	0	<b>0</b>
Efficiency	30 %	2	<b>0.6</b>	1	<b>0.3</b>	0	<b>0</b>	1	<b>0.3</b>
Price	10 %	0	<b>0</b>	1	<b>0.1</b>	1	<b>0.1</b>	0	<b>0</b>
Durability	20 %	0	<b>0</b>	0	<b>0</b>	1	<b>0.2</b>	1	<b>0.2</b>
Sum	100 %	<b>1.4</b>		<b>0.8</b>		<b>0.7</b>		<b>0.5</b>	

In Table 5-1 different gears are compared, and size and efficiency are, as expected, the deciding factors. Compared to alternatives, planetary gears are efficient and compact, and there will be no problems with mounting these inside wheels to obtain a narrow design. It has a slightly higher risk of getting defected because it has more components. Even though the planetary gears are more expensive, they are the preferable choice.

5.2.1 IP STANDARD

Robots should be able to operate in all weather and field conditions. For that reason, making sure that no dust gets inside the gearbox is of great importance. It does not have to be fully waterproof. Important conditions to withstand are rain and muddy ground. IP standards will be discussed further in the chapter where components are selected.

5.2.2 BELT AND PULLEY

In Table 5-2, two types of belts and one transmission with chain are evaluated. The alternatives have about the same compact size, and have therefore gotten the same score. Compared to timing belts and chains, V-belts are considered less efficient because of the risk of slip. Even though chains are made of metal, this option is considered less durable because of its low tolerance for dirt and mud. Timing belts require more precise installation.

Table 5-2: Evaluation of belts and chain

		V-belt		Timing belt		Chain	
Size	40 %	0	<b>0</b>	0	<b>0</b>	0	<b>0</b>
Efficiency	30 %	0	<b>0</b>	1	<b>0.3</b>	1	<b>0.3</b>
Price	10 %	2	<b>0.2</b>	1	<b>0.1</b>	0	<b>0</b>
Durability	20 %	1	<b>0.2</b>	1	<b>0.2</b>	0	<b>0</b>
Sum	100 %	<b>0.4</b>		<b>0.6</b>		<b>0.3</b>	

As a conclusion, the best alternatives are timing belts and planetary gears.

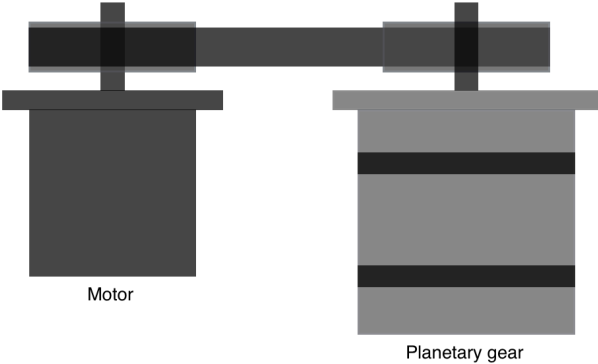


Figure 5-1: Motor and drivetrain example

The gear will be mounted inside the wheel to achieve a narrow construction. To obtain the required reduction ratio for a BLDC motor, the gear will have 2 stages, and the belt will have ratio 1:1. An illustration of the setup of planetary gear, timing belt and motor is shown in Figure 5-1. This setup positions the planetary gear inside the wheel, which provides a low center of gravity. The motor can be outside and above the wheel to make the wheel module narrower, and still be very efficient.

### 5.3 SELECTED COMPONENTS

In building of both Thorvald I and Thorvald II, Electro Drives AS has provided parts with good discounts. They will be a part of the development of Tora as well, and will provide motors and timing belts with pulleys.

#### 5.3.1 MOTOR – 3MEN BL840

3Men Technology was established by three good friends in 1995, hence the name 3Men. This Taiwanese company is specialized in electric motors and drivers [42]. The power needed from each motor is about the same as for Thorvald II. For this reason, the same motors, BL840, will be used. Tora will have two of these motors for propulsion on each front wheel. Motor specifications are listed in Table 5-3, and Figure 5-2 shows a picture of the motor.

Table 5-3: Specifications of BL840

Rated Voltage	48 V
Rated Speed	3000 rpm
Output Power	500 W
Rated Torque	1.57 Nm
Rated Current	12.8 A
Body Length	112.5 mm
Mass moment of inertia	$2.98 \cdot 10^{-4} \text{ kgm}^2$
Weight	3.5 kg



Figure 5-2: Picture of 3Men's BL8 series motor [42]

### 5.3.2 MOTOR CONTROLLER – SBL 1360

Tora will use the same network as before, CANopen, for control. However, because the robot will have propulsion and not steering, there is no need for a motor controller as complex as the one used on Thorvald II, Roboteq FBL2360. In addition, Roboteq FBL2360 has two channels, which is not necessary for this robot, where one motor controller will be located on each wheel module.

The motor controller Roboteq SBL1360 is a controller with one channel capable of a current of 30 A, and it can handle a voltage of 60V. It supports CANopen, and is applicable for automatic guided vehicles. Figure 5-3 shows the Roboteq SBL1360 motor controller.



Figure 5-3: Roboteq SBL1360 [43]

### 5.3.3 PLANETARY GEAR – APEX DYNAMICS AL110

The Apex Dynamics AL110 gear is the same gear used for Thorvald I. This gear is well suited for this application, where the goal is to make the wheel, gear and wheel module width at a minimum. Wheels can be mounted around the gear to make the width narrower than with the gear used on Thorvald II. There have not been any complications with this gear previously. Therefore, no problems can be seen with using this gear. Gear specifications are listed in Table 5-4, and Figure 5-4 shows a picture of the gearbox.



Figure 5-4: Apex Dynamics AL110 planetary gear

The gearbox is designed to withstand a radial load of 6500N, Table 5-4. With the weight of the robot being 200 kg, distributed with approximately 60 kg on each front wheel and 40 kg on each caster wheel, and assuming static conditions, the safety factor is:

$$SF = \frac{6500N}{9.81 \frac{N}{kg} * 60kg} = 11.0$$

The gearbox should be able to handle any shocks it might be exposed to during field operations with a safety factor as high as this.

AL110 is sealed to IP65 standard protection (6 - dust tight, Table 3-1, 5 - protected against water jets, Table 3-2), which means it will handle the conditions discussed in the chapter “IP Standard”. The gearbox is maintenance free, with helical gears ensuring smooth and quiet operation.

**Table 5-4: Specifications for Apex Dynamics AL110**

Number of stages	2
Nominal Output Torque	140 Nm
Emergency Stop Torque	420 Nm
Max. Acceleration Torque	252 Nm
Continuous Input Speed	3000 rpm
Max. Input Speed	8000 rpm
Protection class	IP65
Backlash	$\leq 7$ arcmin
Max. Radial Load	6500 N
Max. Axial Load	3250 N
Efficiency	$\geq 94$ %
Mass Moment of Inertia	0.13 kgcm <sup>2</sup>
Weight	4.1 kg

**5.3.4 TIMING BELT**

As earlier mentioned, a timing belt with ratio 1:1 will be used to transfer power from motor to gearbox in each wheel module. It will spin with high speed and low torque, and, if needed, the ratio can be modified easily by replacing the pulleys with two of different sizes. Design of timing belt with dimensions are shown in Figure 5-5.

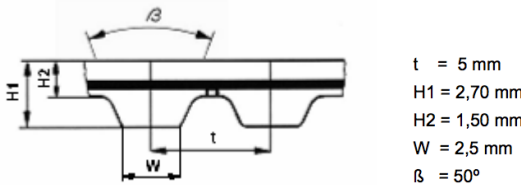


**Figure 5-5: Timing belt [44]**

Illustrations of the pulleys are shown in Figure 5-6, and they are equal in size. According to Semcon Devotek AS [45], to use one pulley with and one without flanges, where the one with flanges are connected to the motor, and the one without flanges are connected to the gear, is common. Semcon Devotek AS stated that if both pulleys were to have flanges, the belt tended to rub against one side of one pulley, and the other side of the other pulley. This would result in the belt wearing out, and it would have to be changed often. If none of the pulleys had flanges, there would be a risk of the belt falling off.

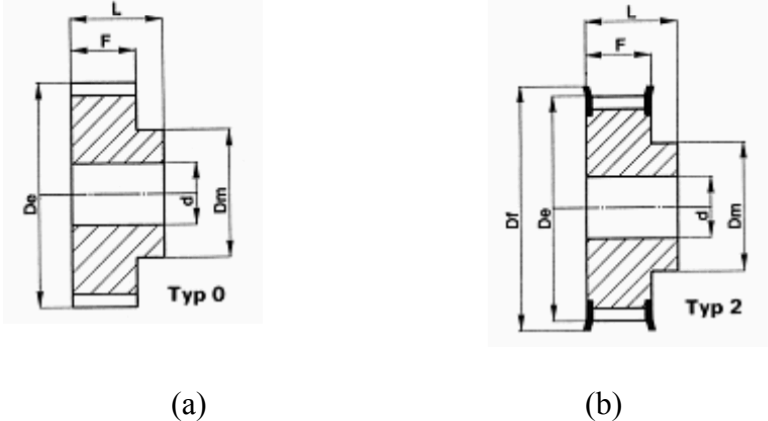


Figure 5-6: Pulleys (a) without flange (b) with flange [44]

Essential specifications of the pulleys are listed in Table 5-5.

**Table 5-5: Pulley specifications**

De	62,45 mm
Number of teeth	40
Weight	138 g

**5.3.5 WHEELS**

A wheel supplier in Norway called Røwdehjul AS was contacted early in the process, and they were very helpful. Røwde delivers complete wheels and wheel components for farming, industry and leisure use all over the country. Today, their assortment is more than 900 components (tires, wheel, hub etc.), and they are Norway’s biggest supplier of tubes and trailer tires [46].

After seeing a wide range of wheels it was eventually decided to use H-271 tire print with diameter 400 mm and width 98 mm [47]. The desirable width of the wheel module with gear and wheel is 150 mm or less, and the wheel module is already about 44 mm wide. The gear was used for Thorvald I, and because of good experiences, the same gear will be used for this robot to keep the wheel, gear and wheel module width to a minimum. Positioning of the wheel can easily be changed if wider wheels are desirable.

From Thorvald I, the fact that the AL110 planetary gears does not fit directly on the wheel and must be modified is known. This is because they are not intended to be used as hub reduction units. To be able to fasten the gear to a wheel, a flange must be machined and fitted to the gearbox output. Holes are drilled in a ring slip-fitted to the gear. The flange will be fastened to the gear with set screws placed 90° apart. A hole in the wheel is extended to fit over the gear, and new holes corresponding to those on the flange are drilled. A spacer is made to get the right position of the gear and wheel module, where there are holes that fit with the flange on the gear and holes that fit the wheel module. Figure 5-8 shows the different parts discussed in this paragraph.

The solution with flange and set screws makes minimal harm to the gearbox, and makes it possible to adjust the wheel's position for perfect alignment with the frame of the robot.

For wheels on the rear end, caster wheels with tire print H-201 is selected, see [47]. The dimensions of these wheels are 270 mm diameter and 86 mm width. For optimal performance, a large diameter is desirable on the caster wheels, and the wheel fork used is one of the largest ones Røwdehjul had in their storage. Figure 5-7 shows the caster wheel with a pipe to give the right height.



**Figure 5-7: Caster wheel**



## 5.4 VERIFICATION OF DRIVETRAIN TORQUE CAPACITY

Each of the two front wheel modules can be presented by the illustration in Figure 5-10, and wheel size, gear ratio and efficiencies are listed in Table 5-6.

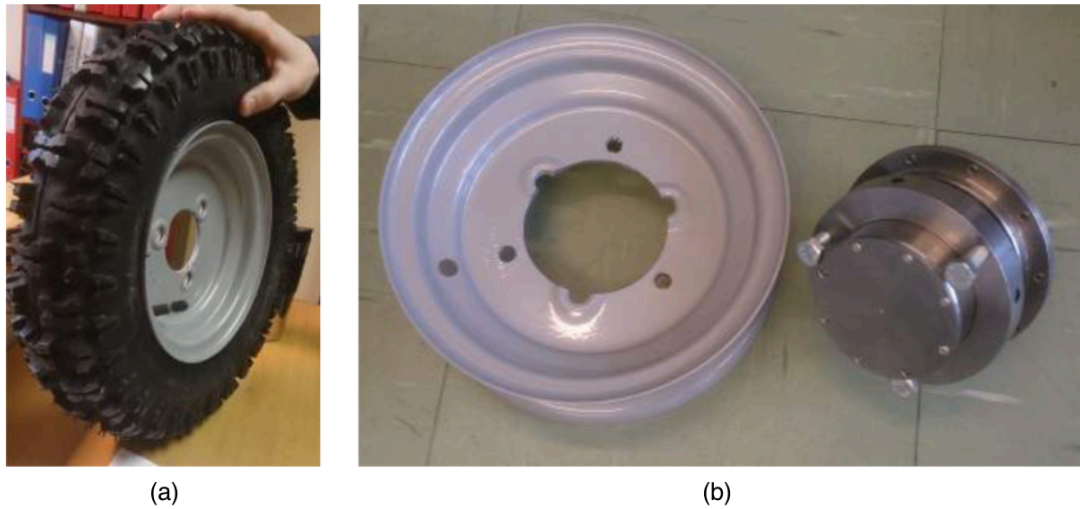


Figure 5-8: (a) Original wheel, (b) Modified wheel and gearbox

A timing belt's efficiency is usually greater than 95 % [48], and will be used for the following calculations. The Apex gearbox has an efficiency of 94%.

An estimate of the required torque per motor at constant speed can be made by multiplying the combined friction forces, from the chapter "Tora Power Requirements", with the radius of the wheel and dividing by the number of wheels with ground contact in addition to each transmissions efficiency and gear ratio:

$$M_A = \frac{563.2 \text{ N} * 0.20 \text{ m}}{2 * 0.95 * 0.94(1 * 60)} = 1.05 \text{ Nm}$$

The power required by each motor can be calculated by dividing required wheel power by overall efficiency of the transmissions:

$$P_A = \frac{422.4 \text{ W}}{0.95 * 0.94} = 473 \text{ W}$$

There might be cases where both caster wheels are locked and work as breaks. In this case, the robot will not be able to drive with the same speed, 1.5 m/s. In Figure 5-9, two cases, one locked wheel and two locked wheels, have been compared.

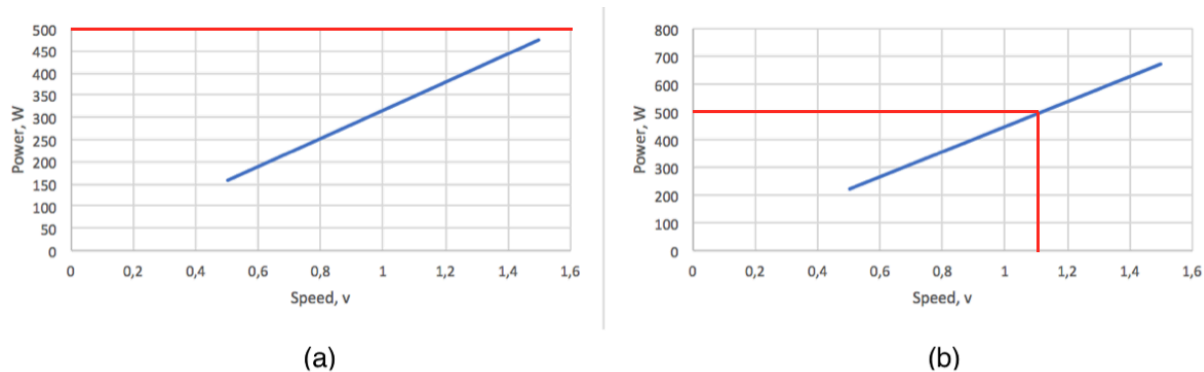


Figure 5-9: Power vs Speed with (a) one wheel locked, and (b) two wheels locked

As can be seen by the red lines in Figure 5-9 (b), the robot will be able to drive with both wheels locked with a speed of about 1.1 m/s. There will therefore not be any cases where the robot will stop completely. It will always get back to its “home”, and there will not be any need for a tractor to drive out in the field and pick it up.

Before calculating the torque needed to accelerate the robot from equation (4-3), the moment of inertia of shaft A, B and C must be calculated, Figure 5-10.

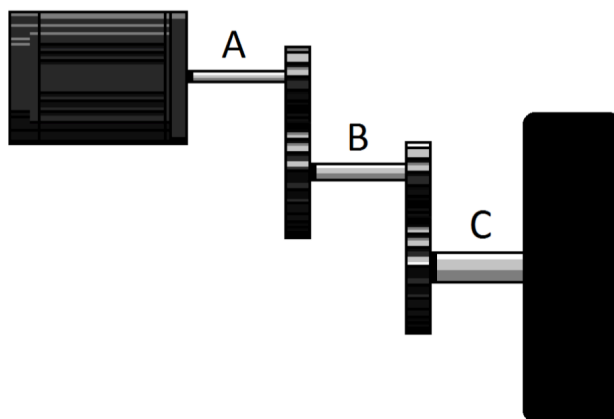


Figure 5-10: Simple drawing of the powertrain

Moment of inertia of Apex Dynamics AL110 gearbox is  $1.3 \times 10^{-5} \text{ kgm}^2$ , see Table 5-4. The pulleys’ moment of inertia is calculated with equation (5-1), and wheels with equation (5-2). The weight of the wheel is approximately 4 kg and the radius is 0.20m [47].

$$I_{cylinder} = \frac{1}{2} m_{cylinder} r_{cylinder}^2 \quad (5-1)$$

Where

$I_{cylinder}$  is the moment of inertia of a cylinder

$m_{cylinder}$  is the mass of a cylinder

$r_{cylinder}$  is the radius of a cylinder

$$I_{thindisc} = \frac{m_{thindisc} r_{thindisc}^2}{2} \quad (5-2)$$

Where

$I_{thindisc}$  is the moment of inertia of a thin disc

$m_{thindisc}$  is the mass of a thin disc

$r_{thindisc}$  is the radius of a thin disc

The shafts in Figure 5-10 is defined as follows:

Shaft A: The motor and the upper pulley

Shaft B: The lower pulley and the gearbox

Shaft C: The wheel

The different moments of inertia, efficiencies and gear ratios are listed in Table 5-6.

An acceleration of approximately  $0.49 \text{ m/s}^2$  is desired for the robot. By having this acceleration, maximum speed can be reached in three seconds. When the wheel radius is  $0.20\text{m}$ , the angular acceleration of the motor shaft will be:

$$\alpha_A = \frac{0.49 \text{ m/s}^2 * 1 * 60}{0.20 \text{ m}} = 147 \text{ s}^{-2}$$

**Table 5-6: Datasheet for the powertrain**

$I_A$	$3.65 \times 10^{-4} \text{ kgm}^2$
$I_B$	$8.03 \times 10^{-5} \text{ kgm}^2$
$I_C$	$0.08 \text{ kgm}^2$
$i_{A-B}$	1
$i_{B-C}$	60
$\eta_{A-B}$	0.95
$\eta_{B-C}$	0.94

By using equation (4-3) with required values, the acceleration torque of the motor is 0.95 Nm. The motor has a rated continuous torque of 1.57 Nm, Table 5-3. By this means, the motor is strong enough to attain the requirements.

The maximum speed of the robot will thus be:

$$\frac{3000 \text{ rpm}}{60} * \frac{\pi \text{ rad/s}}{30 \text{ rpm}} * 0.2 \text{ m} * 3.6 \frac{\text{km/h}}{\text{m/s}} = 3.8 \text{ km/h}$$

## 6 DIMENSIONING OF THE TORA MODULE

A Tora module was built using a Volvo roll cage last summer (2016). The Volvo roll cage was tested on Thorvald II in March with surprising results, Figure 6-1. The module could carry at least two average weight persons. Another test done was positioning all the wheels towards the middle and driving at full speed to see how much the cage would deform. The results were incredible, and showed that the cage was too strong for its application.



Figure 6-1: Strength test of the Tora module

The pipes on each side of the Volvo roll cage are a 45-mm diameter, with 40 mm supporting pipes between. With the test of the cage in mind, and the fact that a light weighted robot is wanted, checking if a lighter version of the module can be used is useful.

The modules have been analyzed in the simulation program ANSYS Workbench 17.2. The module already built, and a modified module with all pipes equal in size, 40 mm diameter, were analyzed. The robot is part of a big project, and being able to use the module for the most powerful robot, four-wheel drive and steering, is therefore preferable. This will be taken into consideration when analyzing the module's strength.

An analysis is performed using two worst case scenarios; 1. wheels driving away from each other, Figure 6-2 (a), 2. wheels driving in opposite directions, on one side wheels drive forward, while on the other side wheels drive backward, Figure 6-2 (b).

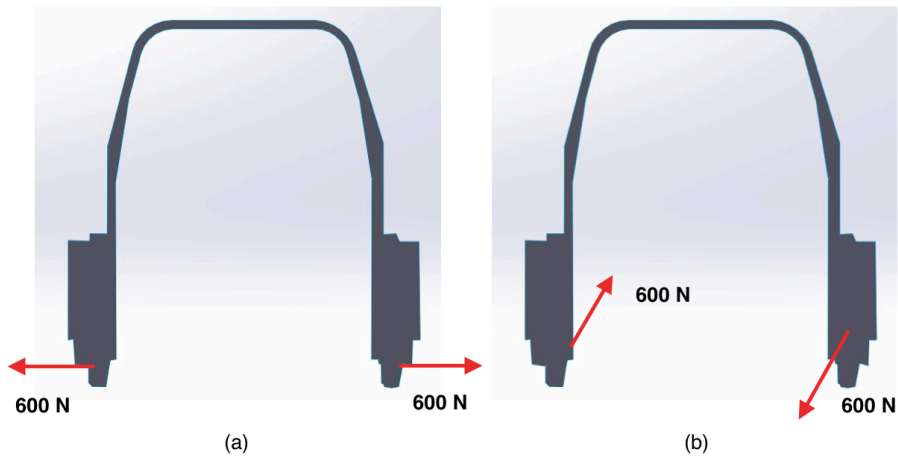


Figure 6-2: Illustration of the scenarios analyzed (a) scenario 1, (b) scenario 2

The total resistance force the motors must overcome is 563 N, Table 4-1. Furthermore, each motor must overcome a force of about 300N. This gives a total of 1200 N when four propulsion motors are applied. For the results to be realistic, scenario 1 has a 1200 N force placed on one side of the module, keeping the other side fixed. For scenario two, one side of the module is fixed, while the other side has a force of 1200 N applied to make the robot rotate. Both scenarios have a 10-kg load on each side of the module that represents spraying equipment, which is the heaviest equipment this robot will carry. The following figures show the equivalent stress and total deformation of the two scenarios.

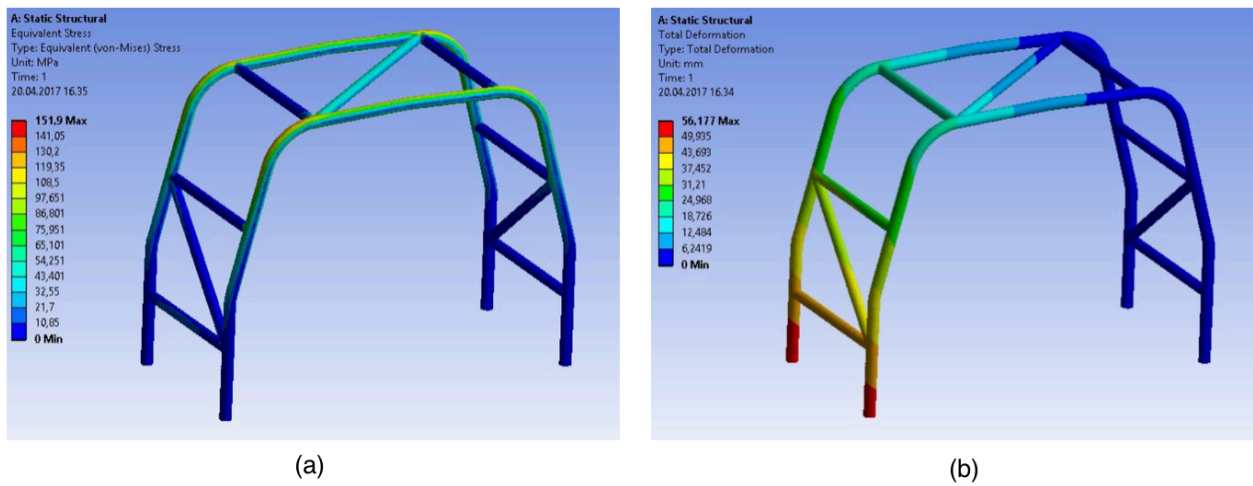


Figure 6-3: ANSYS analysis of the Volvo roll cage with scenario 1; (a) Equivalent stress, (b) Total deformation

Figure 6-3 shows results of the Volvo roll cage with scenario 1. The highest equivalent stress value is 152 MPa, and, as expected, it occurs at each top corner, marked with red. Apart from these areas, the stress rarely exceeds 109 MPa. The total deformation is 5.6 cm. In the simulation, it is located on one side of the module, because one side is fixed. In reality, the deformation would be 2.8 cm on each side.

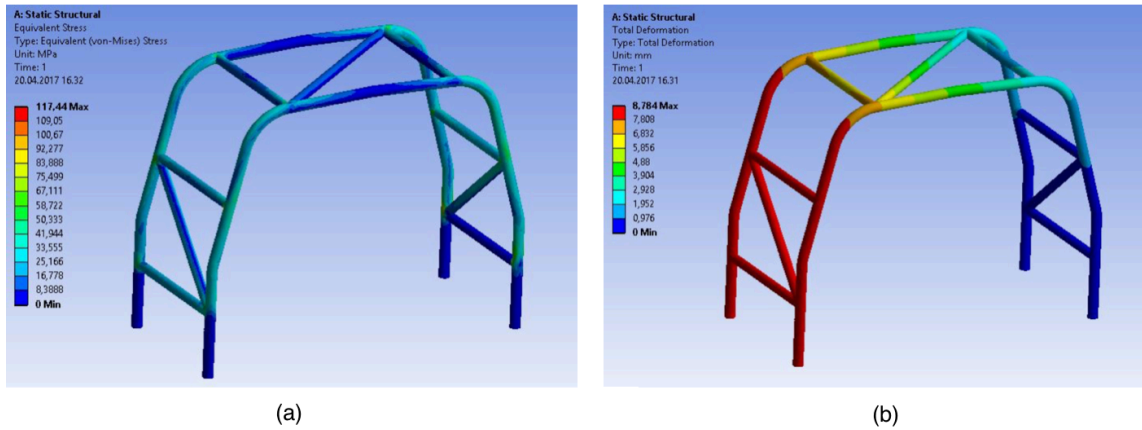


Figure 6-4: ANSYS analysis of the Volvo roll cage with scenario 2; (a) Equivalent stress, (b) Total deformation

Figure 6-4 shows results of the Volvo roll cage with scenario 2. The highest equivalent stress is 117 MPa, and occurs in the intersection points of the module. These points are welded, and therefore have a higher strength than simulations can show. Apart from these areas, the stress rarely exceeds 67 MPa. The total deformation is 8.8 mm, and as in the previous paragraph, this is divided by two to get the value of each side; 4.4 mm.

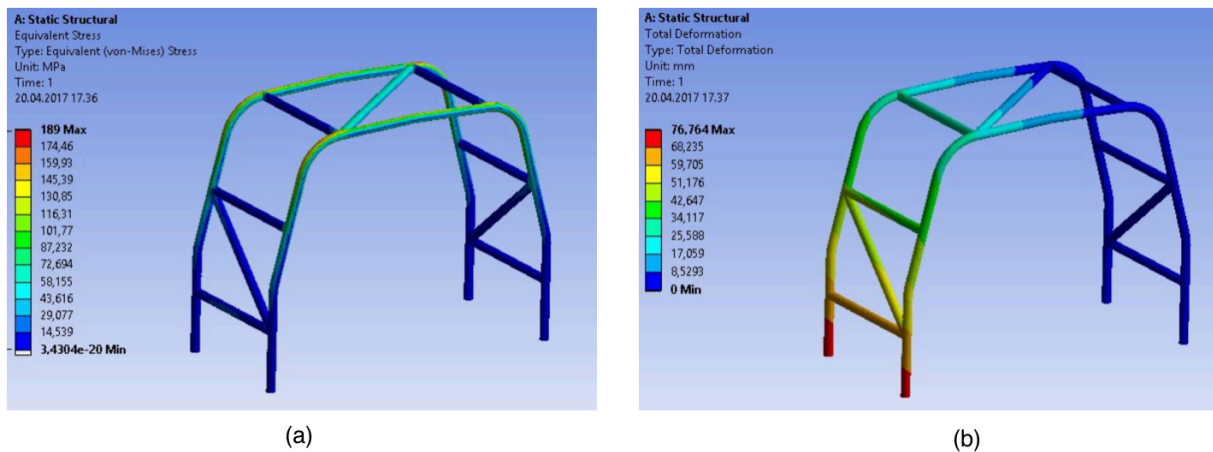


Figure 6-5: ANSYS analysis of the lighter cage with scenario 1; (a) Equivalent stress, (b) Total deformation

Figure 6-5 shows results of a modified module where all pipes are 40 mm in diameter with scenario 1. As expected, the highest equivalent stress is higher than for the Volvo roll cage, about 37 MPa, increased to 189 MPa. The total deformation is about 2 cm greater, and increased to 7.7 cm.

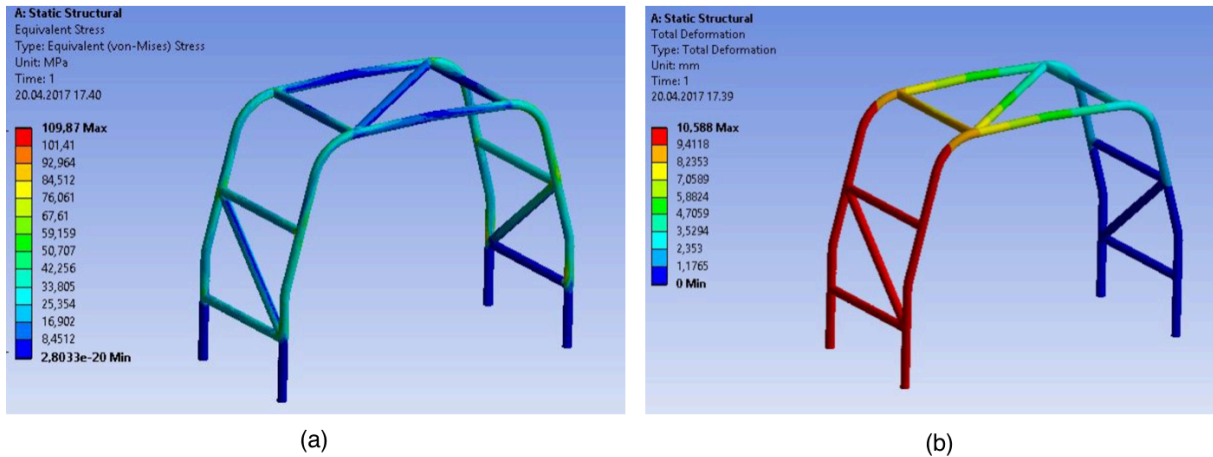


Figure 6-6: ANSYS analysis of the lighter cage with scenario 2; (a) Equivalent stress, (b) Total deformation

Figure 6-6 shows results of a modified module where all pipes are 40 mm in diameter with scenario 2. The highest equivalent stress has decreased by 7 MPa to 110 MPa. The locations of these stress values are, as with the Volvo roll cage, in intersections between the pipes, and is not a reliable value. These points are welded, which makes these areas' strengths increasing. Apart from the intersections, the stress value lies on about 67 MPa, which is the same value as for the Volvo roll cage. The total deformation is 10.6 mm, 1.8 mm more than the Volvo roll cage.

The highest equivalent stress of the new cage occurs at scenario 1, and has the value 189MPa. Knowing this and the fact that the yield stress of the S355 steel cage is 355MPa gives a safety factor of:

$$SF = \frac{355MPa}{189MPa} = 1.88$$

With this safety factor in mind, and knowing that the analysis' are done with worst case scenarios that are as unlikely to happen as these are, the 40-mm new roll cage is applicable.



# 7 WHEEL MODULE MODIFICATIONS

For the wheel modules to be functional with the new gear and wheel, some modifications must be made. The module arm must be designed differently to avoid causing moment and bending of the wheel module. Figure 7-1 shows the differences between the old and new arm.

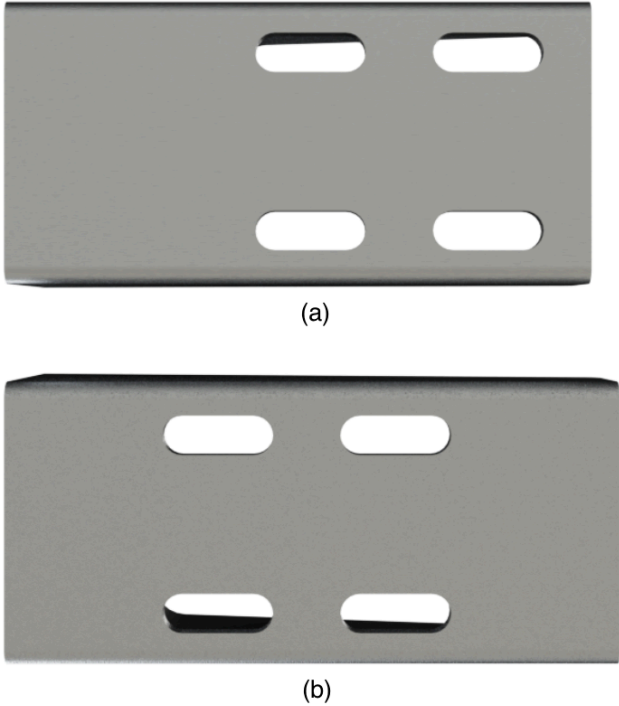


Figure 7-1: (a) Thorvald and (b) Tora wheel module arms

As can be seen in Figure 7-1, the holes are moved closer to the middle of the arm. The arm is extended by 8 mm to be as wide as the motor box, in this way it can be used to fasten the wheel module covers discussed in the next chapter. Figure 7-2 shows the part of the arm where two holes are drilled for the cover to be attached.



Figure 7-2: Tora wheel module arm

A new spacer between the gear and wheel module was also necessary, Figure 7-3. The spacer has been designed to give a right distance between gear and belt pulley. This distance is wanted as small as possible, to obtain a shorter distance between wheel module and wheel.

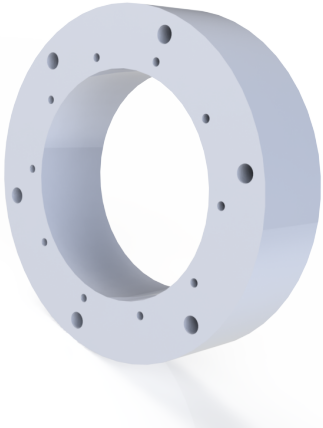


**Figure 7-3: Tora spacer**

It can be seen in Figure 7-3 that two sets of holes are made. The smaller holes are to fasten the gear, and the bigger holes are for the wheel module.

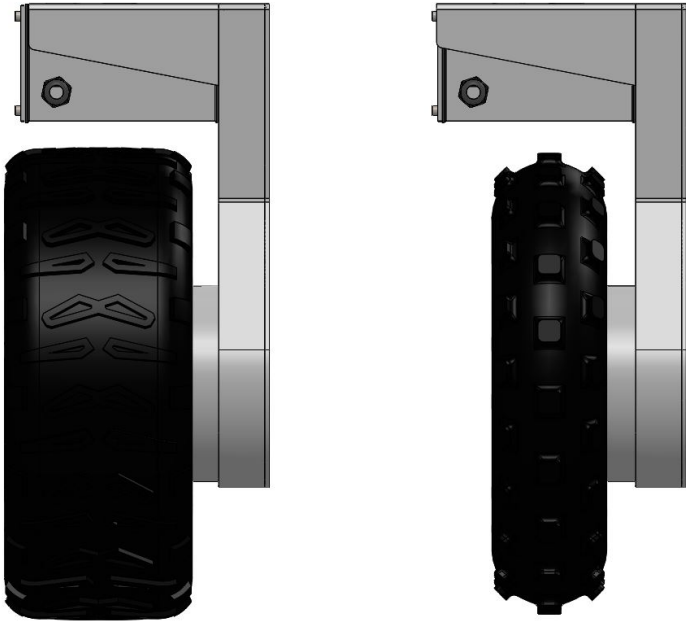


**Figure 7-4: Comparison of Thorvald and Tora wheel modules**

Figure 7-4 compares Thorvald’s and Tora’s wheel modules. As can be seen, the wheel, gear and wheel module width is significantly reduced.

## 8 DESIGN OF COVERS

### 8.1 MATERIALS

Knowing the method of production will help the process of deciding which materials to use. Method of production will be decided based on available equipment. All available equipment at the NMBU workshop can be used, as well as a plasma cutter at the high school in Ås. This is not one of the robots that will be of big production in the near future. For this reason, factors to consider are cheap and efficient ways to produce the parts.

The weight of the robot is one of the most important factors for this project. The project demands low weights to avoid soil compaction, as discussed in the chapter “The Thorvald Project”. Aluminum has a third of the weight of steel. If assembled right, aluminum constructions can have the same strength as a steel construction with a much lighter weight. With aluminum, a sheet that is three times thicker than a sheet of steel can be used and still have the same weight. Having a thickness on the sheets makes the covers stronger against buckling. For this reason, aluminum will be chosen over steel. Aluminum is isotropic, which means that the material has the same characteristics in every direction.

One option that is easy and available is plasma cutting and bending of aluminum sheets. Aluminum sheets can easily be bent into desired shapes. This is an inexpensive method to use, and since NMBU’s workshop have a machine that can bend the sheets, and the high school in Ås has a plasma cutter, no extra equipment is needed.

Composites like fiberglass have also been considered. Composites are orthotropic, which means that they are stronger in the direction of the fibers and weaker in the direction perpendicular to the fibers. This material requires molding, where a mold needs to be produced to form the fiberglass, see the chapter “Composite”. This is a more time-consuming process. An oven big enough for the cover with mold is needed for the molding process.

The design must protect materials from corrosion. For aluminum components powder-coating, which is highly resistant to corrosion can be used. Aluminum can also be anodized to protect it from corrosion.

### 8.2 ASSEMBLY TECHNIQUE

The main assembly technique used for Thorvald I was glue, because of the availability. This assembly technique did not hold, and the frame had to be bolted even though it was not designed for this method. With this incident in mind, Thorvald II was mainly using welding and bolting for steel components, and riveting for aluminum components.

The adhesive Araldite AW4858 with hardener HW4858 [49] was tested spring 2017. For this robot’s purpose, glue would be ideal to avoid bolts and sharp edges for grains to get stuck on. Test pieces were abraded with sandpaper grit 180 and cleaned with isopropanol before they were glued. The glue had to be cured for 16 hours at 40°C, and was tested at about 23°C. In absence of oven alternatives for curing, a sauna was used for the curing process, see Figure 8-1.



Figure 8-1: Curing in a sauna. Image: Remy Zakaria

The tests showed promising results, Table 8-1, and will be used on the parts of the cover where no reassembling are necessary or strong forces are applied. The glue was tested for cleave, strain and shear, and Figure 8-2 shows some pictures from the test days.

Table 8-1: Test results of the adhesive Araldite AW4858 with hardener HW4858 [50]

<b>L(Cleave)</b>				
Treatment	A(mm <sup>2</sup> )	F(N)	MPa	
Unhardened	472.8	1899	4.0	Adhesion
Unknown	477.8	3069	6.4	Adhesion
Unknown	477.8	3003	6.3	Adhesion
Hardened	477.8	2525	5.3	Adhesion
Hardened	477.8	2260	4.7	Adhesion
Average	476.8	2551.2	5.4	

<b>T(Strain)</b>				
Treatment	A(mm <sup>2</sup> )	F(N)	MPa	
Unhardened	520	3885	7.5	Cohesion
Hardened	455	4144	9.1	50/50
Hardened	487.5	2596	5.3	Cohesion
Average	487.5	3541.7	7.3	

<b>I(Shear)</b>				
Treatment	A(mm <sup>2</sup> )	F(N)	MPa	
Unhardened	187.2	2906	15.5	Cohesion
Hardened	188.5	3668	19.5	50/50
Hardened	153.3	3005	19.6	Cohesion
Hardened	201.6	4243	21.0	Cohesion
Hardened	171.3	3789	22.1	50/50
Average	180.4	3522.2	19.5	

All the glue areas on the robot will be placed parallel with the forces, which makes shear the most relevant results for application on this robot. Especially for shear, the results indicate a need for hardening. From the tests and results came knowledge; factors of great importance are:

- Use of fresh glue (initial hardening was faster than expected)
- Use of perfectly abraded pieces
- Use of fully degreased surfaces.



Figure 8-2: Test days [50]

For most of the assembling of the cover, bolts will be used. Bolts is the ideal technique to use because of its ability to disassemble if necessary.

### 8.3 WHEEL COVERS

Early developments of covers had sketches of covers in one piece. Furthermore, as the covers should be functional for a robot with steering as well, a decision of making a separate cover for wheel modules and a cover for the rest of the robot was made. When grains are short, they stand tall. But, as they grow taller, they tend to sag, and this is when covers are needed. Caster wheels must be able to rotate freely, and since the top cover will take care of grains when they grow tall, covers on the caster wheels are not necessary.

When designing the covers, three different shapes were in mind; round shape, triangle shape, and pipes.

#### 8.3.1 ROUND

For the round shape, inspiration is gathered from the covers of airplane wheels, see Figure 8-3. A material often used for shapes like this is fiberglass, which is a lightweight material with properties from both glass fibers that are strong and stiff, and polymers that are flexible. See the chapter “Composites” to read more about composites and this material.



Figure 8-3: Covers airplane wheels [51]

A round shape, Figure 8-4, might not be ideal. Without testing, the decision is hard to make. With no knowledge of grain behavior, it is hard to tell whether round covers will separate grains or break them off. Another difficulty is knowing which direction grains will move when facing the covers. They might end up under the cover and wheel as the arrows in Figure 8-4 show.

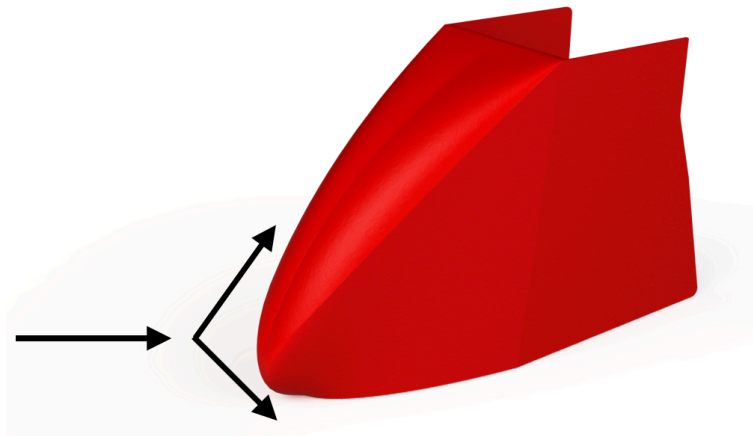


Figure 8-4: Round cover

### 8.3.2 TRIANGLE

Triangle shapes, or straight shapes in general, are a lot easier to deal with. This often leads to it being cheaper than the alternatives. Bending would be an ideal production method, with equipment available at the NMBU workshop. Bending of sheet metal is an easy and inexpensive production method. Low weight is required, which makes aluminum an ideal material. The triangle shape, Figure 8-5, is sloping upward with a sharp tip at the bottom. The tip will easily find its way between grains, and the slope will push grains upward until they eventually separate.

The first triangle cover made, Figure 8-5 (a), had a very sharp edge in front. This resulted in concerns on whether the cover would divide or cut the grains. This concern started the process of designing the second cover, see Figure 8-5 (b). This cover has more edges, and is not as sharp as the first one.



**Figure 8-5: Triangle covers. (a) Three bends, (b) Five bends**

### 8.3.3 PIPES

Pipes instead of metal sheets and composites have also been an alternative. For this method, aluminum pipes would be welded together in front of the wheels to make a triangle shape. The clamps that are used for the pipes, replaced by the Tora-module, can be used to fasten the “pipe cover”. The idea was to bend the pipes so that they follow the electric box on each side down to the wheel module, 15 cm above ground. From here, they would get bent and make a tip in front of the wheels. A pipe will also go from this tip and slope upwards in front of the wheel. This pipe would be the divider of the grains, and the pipes on each side of the wheels would be rails guiding the grains around the robot.

This shape will make the total robot wider. The clamps are made for pipes with a 40-mm diameter, and 40 mm pipes are therefore the only option. This would make each side of the robot 80 mm wider than it already is. As mentioned earlier; the goal is to keep the robot slim, which is not achieved with pipes.



## 8.4 COVER ANGLE

As can be seen in “Figure 1-1”, equipment that deals with grains today has a gentle slope of 30 degrees, which was confirmed by the workers at Vollebekk research farm.



Figure 8-6: Grain harvesting equipment. Image: Kristine Skattum

If this robot were to have a gentle slope like this, the covers would almost have the same length as the robot itself. Figure 8-7 shows an illustration of the cover with 30° angle. This is an angle that is known to do the task separating grains, which is a huge advantage. The robot would need a big space to turn with a nose like this.

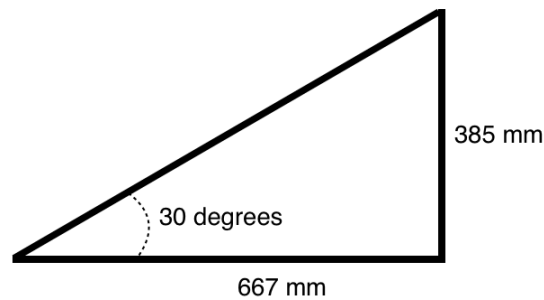


Figure 8-7: Illustration of cover with 30 degrees slope

Figure 8-8 shows an alternative where the angle is increased to 60°. To say if this will work without testing it in the field is impossible. With a sharp angle like this, there is a risk of cutting grains instead of separating them. This will be taken into consideration when selecting a cover.

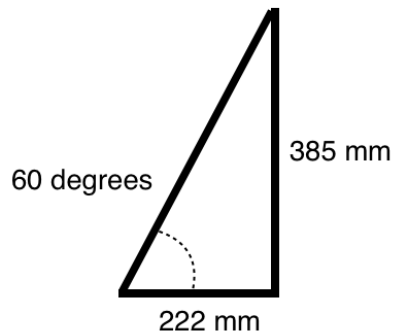


Figure 8-8: Illustration of cover with 60 degrees slope

## 8.5 COVER SELECTION

### 8.5.1 SHAPE

Important factors for cover selection should be defined, to make the decision process easier. As stated in the chapter “Requirements”, among other requirements the need for a slimmer robot and low weight is of great importance when selecting covers. The robot should be able to drive in between the squares of grains, see Figure 3-1, without making any damage on grains. Width is therefore given 40 %. Time is a limiting factor, which makes availability and production time factors of great importance, 20% each. Further the requirement of keeping the weight as low as possible is important, but this decision cannot come at the cost of other important factors, and is therefore given 10 %. Keeping the price as low as possible is always desirable, but there are other factors that are more fundamental, 10 %.

Table 8-2: Evaluation of Covers

		Round		Triangle		Pipes	
Width	40 %	1	<b>0.4</b>	1	<b>0.4</b>	0	<b>0</b>
Weight	10 %	2	<b>0.2</b>	1	<b>0.1</b>	0	<b>0</b>
Price	10 %	0	<b>0</b>	0	<b>0</b>	0	<b>0</b>
Production Time	20%	0	<b>0</b>	1	<b>0.2</b>	1	<b>0.2</b>
Availability	20 %	0	<b>0</b>	0	<b>0</b>	0	<b>0</b>
Sum	100 %		<b>0.6</b>		<b>0.7</b>		<b>0.2</b>

In Table 8-2, the different covers are compared. When comparing the alternatives, the differences between round and triangle shape are minimal. The triangle shape “won” with a small margin. Because of this, available equipment will be the deciding factor. For the round cover, a mold must be made before forming of the shape can take place. In the molding process an oven big enough to fit the covers is needed. For a triangle cover of aluminum, a plasma cutter is available at the high school in Ås, and a bending machine is available at NMBU’s workshop. With this in mind, in addition to the fact that the deadline is near, the triangle shape is the desirable.

**8.5.2 COVER ANGLE**

One important factor to examine when designing covers for separation of grains, is the angle of the covers. When evaluating cover angle, there are two factors of higher importance than others; grain functionality and robot functionality. If the cover does not separate the grains, and rather cuts the grains, the cover loses its function. If the cover does not work on a robot, it also loses its function. These two factors have therefore gotten the highest percentages of importance, 30%, see Table 8-3. Another factor to consider is length, where the cover loses its function if the length is too long and the risk of hooking grains is high, 20%. The two last conditions to consider are weight and price. These two factors cannot come at the cost of low functionality and is therefore given the lowest percentage, 10%.

**Table 8-3: Evaluation of cover angle**

		30°		60°	
Length	20 %	0	<b>0</b>	1	<b>0.2</b>
Weight	10 %	0	<b>0</b>	1	<b>0.1</b>
Price	10 %	0	<b>0</b>	1	<b>0.1</b>
Grain functionality	30%	1	<b>0.3</b>	0	<b>0</b>
Robot functionality	30 %	0	<b>0</b>	1	<b>0.3</b>
Sum	100 %	<b>0.3</b>		<b>0.7</b>	

Table 8-3 shows a superior victory to the 60° angle. Grain functionality is the only property where the 30° angle won. Grain functionality is of great importance to the project, and even though the 60° angle won and will be selected when designing. This will be discussed further in the discussion chapter to make sure the 60° angle is more capable of separating grains without damaging when mounted on a robot.

After several thoughts and designs, the covers are now separated into four part;

- Wheel module cover, Figure 8-9 (a)
- Side cover, Figure 8-9 (b)
- Front cover, Figure 8-9 (c)
- Back cover, Figure 8-9 (d)

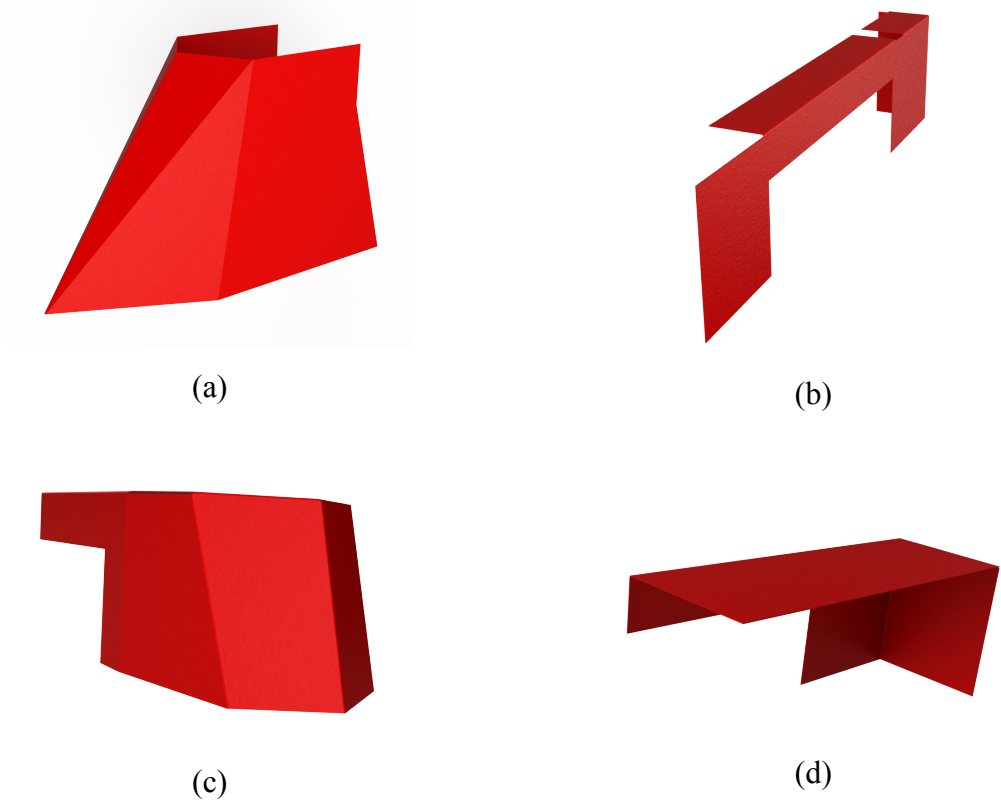


Figure 8-9: Cover parts (a) Wheel module cover, (b) Inside cover, (c) Front cover, and (d) Back cover

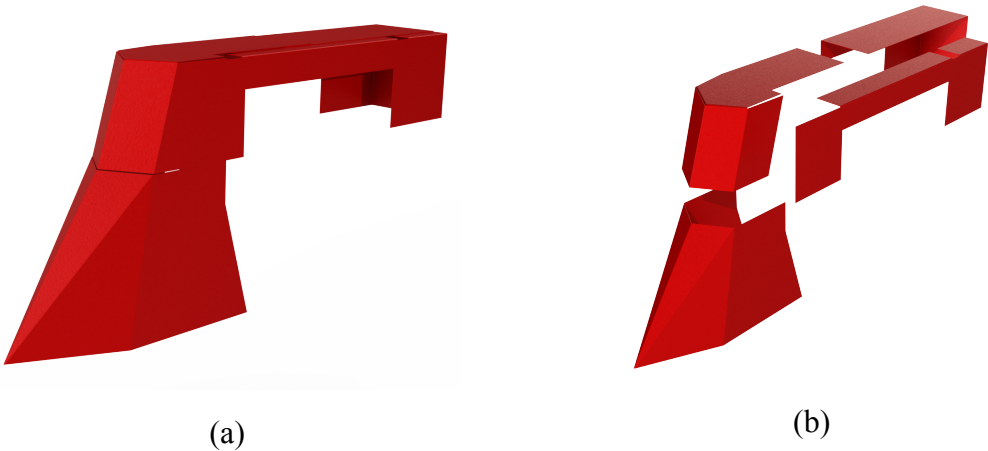


Figure 8-10: Covers (a) Assembled, (b) Exploded view

## 9 DISCUSSION

The thesis shows signs of the time limit of four months. Components were selected based on previous work, and the outcome might have been different if there were more time available. The Thorvald project have a lot of contacts, which were used for this project as well.

Component selection was therefore a process started at an early stage. Other companies were also contacted, but dialogs were better with companies that already knew about the project, and could relate to it. There might be better solutions on the market, but with limiting time, using cooperative companies was the best solution.

Pugh's method is used to select designs and components. This is a method where a decision matrix helps the selection process. Knowing that this method only forms an indication of the best result is of great importance, and being critical to the results is important in making sure that the best solution is being made. In selections where the scores compared have large gaps, the results are more convincing than when the best solution won with a small margin. By this means, results with small margins have been discussed further to make sure that the best solution is made in the end.

### 9.1 STEERING

Applications like phenotyping research does not require as much power as heavier agricultural work. Flat fields will be the only application area. Obstacles that the robot might face are bad weather, wind, and muddy ground.

Prior to this thesis, the decision of using two-wheel drive with differential steering was made. Knowing all obstacles and the fact that the robot will have two-wheel drive, power calculations showed that the motors used for Thorvald II were strong enough. Even though calculations indicate that the robot has enough power with two-wheel drive and caster wheels, there are some concerns with using caster wheels. On rainy days, when grounds are muddy, caster wheels' behavior is impossible to tell. But, the power calculations show that the robot can drive even with both caster wheels locked.

Caster wheels are predictable when used on flat floors or roads, as concrete, asphalt etc., but when placed out in a field, their movements are unpredictable. A question that can have big consequences in a phenotyping field arises; will the caster wheels be stable and handle the terrain in the field, or will a bump in the road cause the robot to turn where it is not supposed to? If the robot turns where it is not supposed to, the risk of hooking grains increases, and the robot's functionality is weakened.

Another solution would be to use four-wheel drive with skid steering, where each side is actuating at different rates or in different directions, causing the wheels to slip, or skid, on the ground. This would result in a more expensive and heavy robot, because additional motors and gears are needed. But as price and weight is of less importance and skid might be a better solution for phenotyping fields, it should be discussed further.

With skid steering, the concern with unpredictable movements are solved. No wheels will rotate freely. This gives the opportunity of having covers on the rear end of the robot as well. With this adjustment, the robot will be more convincing in the way of separating and not driving over grains. The robot will be able to rotate on the spot, which is a big advantage when space is limiting.

When discussing steering, four-wheel drive and four-wheel steering should also be considered. The covers have been designed for use on this version as well, but is four-wheel steering suitable for the phenotyping field? With four-wheel steering, the robot can rotate on the spot without making deep tracks in the field, which will occur with skid steering. As the four-wheel steering causes the whole wheel cover to turn, the risk of hooking increases. Every time the robot makes a small steering adjustment, the cover also makes a small turn. With the small clearance between the grain squares, the covers will hook grains and cause the robot to drive over them.

## 9.2 TORA MODULE

The ANSYS analysis performed in chapter “DIMENSIONING OF THE TORA MODULE” shows that the dimensions of the Volvo roll cage are more than strong enough for its applications. The analysis is performed using a Thorvald with four-wheel drive and worst case scenarios. Even a cage with all pipes being 40 mm diameter are strong enough for the application on a four-wheel drive Thorvald. From these results, questions arise on whether to use the one already made, or make a new one with 40 mm diameter.

On one hand, Tora would be lighter with new dimensions, but on the other hand it would be less time consuming using one already built. All pipes used on standard parts of Thorvald are 40 mm in diameter. With 40-mm diameter pipes on the cage, there would not be a need for special designed t-clamps to hold the pipes together. But, the cost of producing a new cage contra producing the clamps are higher. The Volvo roll cage should therefore be used in this case, but if built in the future, the cage should be dimensioned with all the pipes being 40 mm in diameter.

## 9.3 WHEEL COVERS

One of the requirements from Vollebekk research farm was a cover angle of 30°. As stated in the chapter “Cover Angle”, a cover with 60° angle is selected instead. For a big heavy tractor, an angle of 30° is perfect. The cover weight is almost zero compared to the tractor weight. The same can be said about the length of the cover.

As this is a small robot, where weight is a fundamental value, a cover with a 30° angle is not preferable. To make sure that the robot separates the grains without damaging them, other precautions have been made. With the chosen shape, triangle, the first design had one sharp edge instead of multiple less sharp edges. The new design has multiple edges to adjust the sharpness of the cover, which makes it more reliable. For the cover's applications, separating grains, it is proven from practical experience that the 30° covers work, but on the other hand, it is not proven that the 60° covers will not work.

Separating grains with a tractor is only necessary when harvesting grains. At this point the only purpose is leading the grains into a harvesting tool mounted on the tractor. For this reason, positioning is not as important as for this project. The purpose of the robot with covers in this project is to drive in the lanes between the squares of grains without causing damage on the grains. High precision is therefore of great importance. As robots regulate their position all the time, an angle of 30° would not be a preferable solution. With a long "nose" like this in front of the wheels, the risk of hooking grains and driving over them instead of pushing them away is high. With a longer arm, one small steering adjustment makes a huge difference on the tip of the arm.

## 10 CONCLUSION

The goals of this thesis were very ambitious, where time was the biggest obstacle. When this thesis is sent to printing, there is a lot remaining. The production of covers and machined parts has not started yet, but all the selected components are ordered. Hopefully, some of the parts will be done when defending takes place.

A lot of requirements were set to this thesis, see the chapter “Requirements”, and the goal of fulfilling all of them were quite ambitious. As expected some of the standard parts of Thorvald had to be replaced to fulfill all the requirements from Vollebekk research farm. Having a cover angle of 30°, as the covers on tractors have, was not possible because of the many differences between a robot and a tractor. These changes are small, and the conclusion is therefore that all requirements have been fulfilled to a certain extent.

With the modifications made in mind, the robot will function better than last year. The wheel is narrower, the robot is taller, and covers are made to separate the grains when they tangle. If the results from testing look promising, the robot is ready for the phenotyping field. If not, new modifications should be made with following tests.

To obtain optimal functionality of the robot, the next version should implement the following changes;

- Skid steering instead of differential steering
- Use smaller dimensions on the Tora module, 40 mm pipes



## 11 BIBLIOGRAPHY

- [1] J. K. Brodin, "Forskere lager nye plantesorter ved hjelp av robot," 2017.
- [2] S. Pugh, *Total design: integrated methods for successful product engineering*. Addison-Wesley, 1991.
- [3] L. Grimstad, "Powertrain, Steering and Control Components for the NMBU Agricultural Mobile Robotic Platform," Master's Thesis, Norwegian University of Life Sciences, 2014.
- [4] F. Blomberg, "Frame construction for autonomous agriculture machine," Master's thesis, Norwegian University of Life Sciences, 2014.
- [5] M. Austad, "Powertrain and Steering Modules for the NMBU Agricultural Robot," Master's Thesis, Norwegian University of Life Sciences, 2016.
- [6] Ø. T. Sund, "Chassis Modular Design and Electrical Layout for the NMBU Agricultural Robot Project," Master's Thesis, Norwegian University of Life Sciences, 2016.
- [7] ACPFG. *The Phenotyping Group at ACPFG*. Available: <http://www.acpfg.com.au/index.php?id=120>
- [8] S. Sankaran *et al.* (2015). *Advances in Field-Based High-throughput Phenotyping and Data Management: Grains and Specialty Crops*. Available: [https://nifa.usda.gov/sites/default/files/resources/Advances in Field-Based High-throughput Phenotyping and Data Management.pdf](https://nifa.usda.gov/sites/default/files/resources/Advances%20in%20Field-Based%20High-throughput%20Phenotyping%20and%20Data%20Management.pdf)
- [9] G. Terjesen, "Spenningsanalyse og trykkbeholdere," 2016.
- [10] R. C. Hibbeler, Pearson, Ed. *Mechanics of Materials*, 8. edition ed. 2011.
- [11] www-materials.eng.cam.ac.uk. *Specific stiffness - Specific strength*. Available: [http://www-materials.eng.cam.ac.uk/mpsite/interactive\\_charts/spec-spec/NS6Chart.html](http://www-materials.eng.cam.ac.uk/mpsite/interactive_charts/spec-spec/NS6Chart.html)
- [12] W. D. Callister JR and D. G. Rethwisch, J. W. Sons, Ed. *Materials Science and Engineering*, 9 ed. 2011.
- [13] MartinDiehl. (2013). *Crystal lattice*. Available: <https://damask.mpie.de/Documentation/CrystalLattice>
- [14] CompositeWorld. *Fabrication methods*. Available: <http://www.compositesworld.com/>
- [15] D. A. Smith, *Die design handbook*. Society of Manufacturing Engineers, 1990.
- [16] S. Ramakrishnan and M. Rogozinski, "Properties of electric arc plasma for metal cutting," *Journal of Physics D: Applied Physics*, vol. 30, no. 4, p. 636, 1997.
- [17] A. Iosub, G. Nagit, and F. Negoescu, "Plasma cutting of composite materials," *International Journal of Material Forming*, vol. 1, no. 1, pp. 1347-1350, 2008.
- [18] I. Skeist, *Handbook of adhesives*. Springer Science & Business Media, 2012.
- [19] D. A. Fanella, R. Amon, B. Knobloch, and A. Mazumder, "Bolts and Rivets," in *Steel Design for Engineers and Architects*: Springer, 1992, pp. 186-230.
- [20] J. M. Hughes. *Tool Techniques*. Available: <https://www.safaribooksonline.com/library/view/practical-electronics-components/9781449373221/ch04.html>
- [21] J. Y. Wong, *Theory of ground vehicles*. 2008.

- [22] M. Webster. (1828). *On-line dictionary*. Available: <https://www.merriam-webster.com/>
- [23] M. Motor. *Maxon Motor online product catalog*. Available: <http://www.maxonmotor.com/maxon/view/catalog/>
- [24] Siemens. *SIMOTICS HV Series High Speed* Available: <http://www.industry.siemens.com/drives/global/en/motor/high-voltage-motors/synchronous-motors/specialized-motors/Pages/specialized-motors.aspx>
- [25] B. J. Chalmers, *Electric motor handbook*. Elsevier, 2013.
- [26] R. Condit, "Brushed DC Motor Fundamentals," *Microchip Technology Inc*, <http://ww1.microchip.com/downloads/en/AppNotes/00905a.pdf>, 2004.
- [27] D. Collins. (2016). *FAQ: How can brush wear in DC motors be minimized?* Available: <http://www.motioncontroltips.com/faq-how-can-brush-wear-in-dc-motors-be-minimized/>
- [28] P. Yedamale, "Brushless DC (BLDC) motor fundamentals," *Microchip Technology Inc*, vol. 20, pp. 3-15, 2003.
- [29] TheEditorsOfEncyclopædiaBritannica. *Transmission*. Available: <https://global.britannica.com/technology/transmission-engineering>
- [30] GribbsGears. *Gear Types*. Available: <http://www.gibbsgears.com/>
- [31] Hewitt&Topham. *Gear specialists*. Available: <http://www.hewitt-topham.co.uk/>
- [32] D. Walton. *Martin Gear manual*. Available: <http://www.martinsprocket.com/docs/default-source/brochures---gears/martin-gear-manual.pdf?sfvrsn=14>
- [33] NationalElectricalManufacturersAssociation, "NEMA Enclosure Types ", Available: <https://www.nema.org/Products/Documents/nema-enclosure-types.pdf>
- [34] R. Perneder and I. Osborne, *Handbook Timing Belts: Principles, Calculations, Applications*. Springer Science & Business Media, 2012.
- [35] A. K. Srivastava, C. E. Goering, R. P. Rohrbach, and D. R. Buckmaster, *Engineering principles of agricultural machines*. American society of agricultural engineers, 1993.
- [36] D. S. Murali. (2015). *Power transmission by belts*. Available: <https://www.slideshare.net/smuralichinna/unit-2b-power-transmission-by-belts>
- [37] P. E. Sandin, "Robot Mechanisms and Mechanical devices," 2003.
- [38] PfeiferIndustries. *Timing Belt Tooth Profiles and Pitches*. Available: <http://www.pfeiferindustries.com/timing-belt-tooth-profiles-pitches-i-17-1-en.html>
- [39] R. Nave. *Friction*. Available: <http://hyperphysics.phy-astr.gsu.edu/hbase/frict.html>
- [40] G. Terjesen, "Grunnlag drivkraftteori TMP 270," 2014.
- [41] HPWizard. *Tire-road characteristics*. Available: <http://hpwizard.com/tire-friction-coefficient.html>
- [42] 3Men. *Brushless DC motor*. Available: [http://www.3men.com.tw/style/frame/m1/frame.asp?lang=2&customer\\_id=2958&content\\_set=color\\_3](http://www.3men.com.tw/style/frame/m1/frame.asp?lang=2&customer_id=2958&content_set=color_3)

- [43] Roboteq. *SBL13XX*. Available: <http://www.roboteq.com/index.php/docman/motor-controllers-documents-and-files/documentation/datasheets/sbl13xx-datasheet/61-sbl13xx-datasheet/file>
- [44] Transtech, "AT5."
- [45] "Pulleys," ed: Semcon Devotek AS, 2017.
- [46] Røwdehjul. *Din totalleverandør av komplette hjul*. Available: <http://rowde.no/>
- [47] Røwdehjul. (2016). *Rowdekatalog*. Available: <http://rowde.no/filer/Rowdekatalog2016.pdf>
- [48] SDP/SI, "Handbook of Timing Belts, Pulleys, Chains and Sprockets."
- [49] Huntsman. *Araldite AW4858/ Hardener HW4858*. Available: <https://www.galindberg.se/media/1356/araldite-aw4858-hardener-hw4858.pdf>
- [50] K. Skattum and R. Zakaria, "Araldite AW4858," Huntsman, Ed., ed, 2017.
- [51] Seabee. *Cessna 206H Stationair 2000 model*. Available: [http://www.seabee.info/noah/cessna\\_206.htm](http://www.seabee.info/noah/cessna_206.htm)

## 12 APPENDIX

- Construction drawings. 7 pcs.

The drawings are made with extra files for plasma-cutter and bending machine, all measurements are therefore not present.

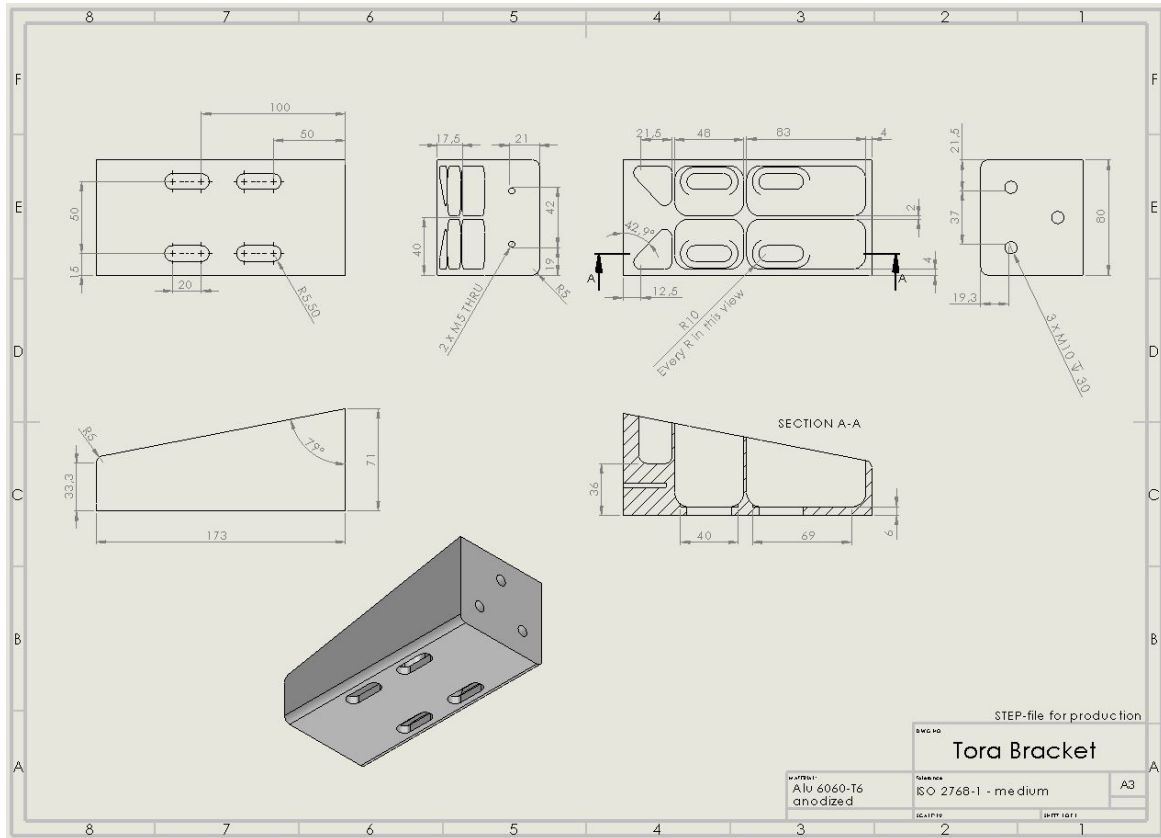


Figure 12-1: Construction drawings of the wheel module arm

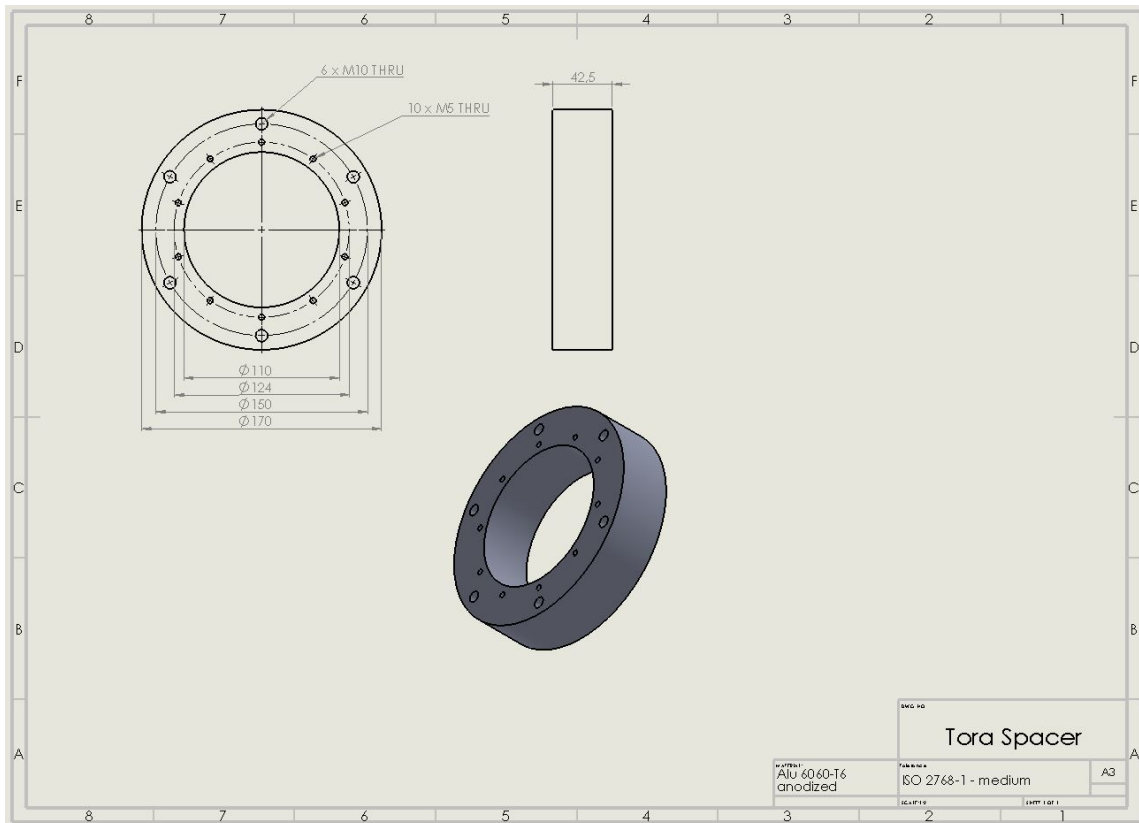


Figure 12-2: Construction drawing of the wheel spacer

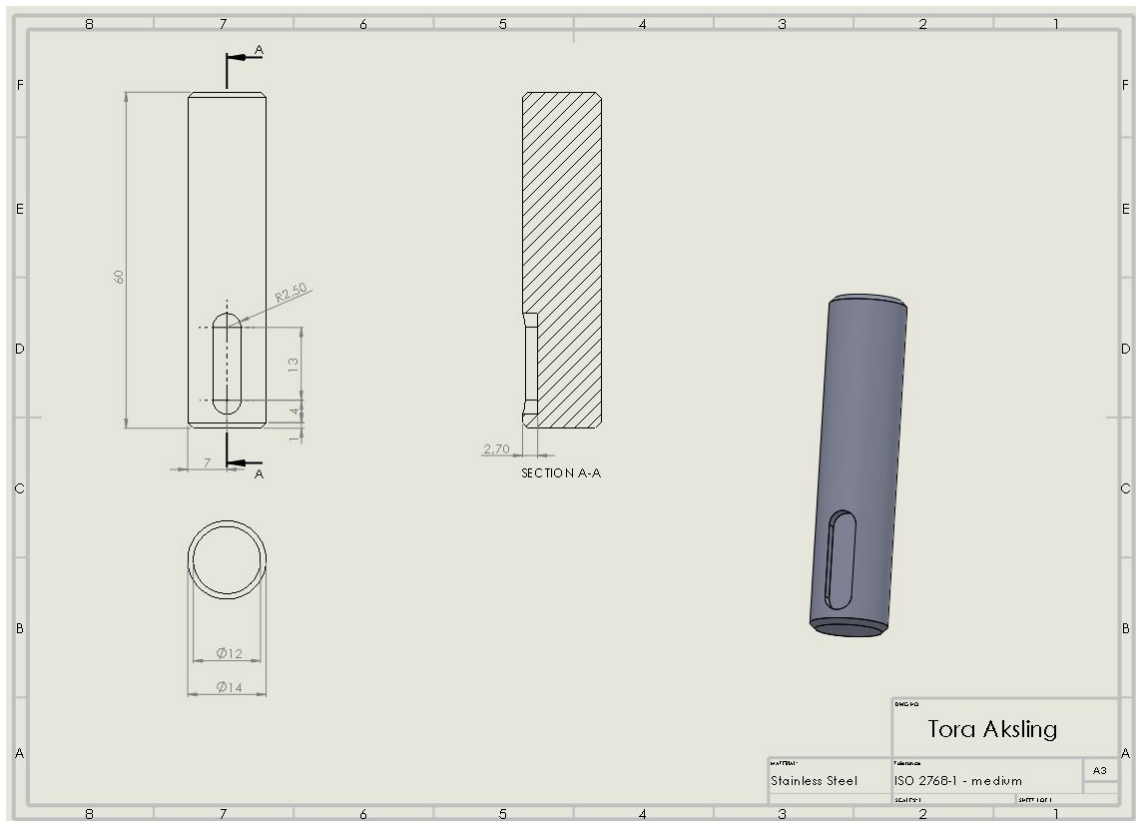


Figure 12-3: Construction drawing of the gear axle

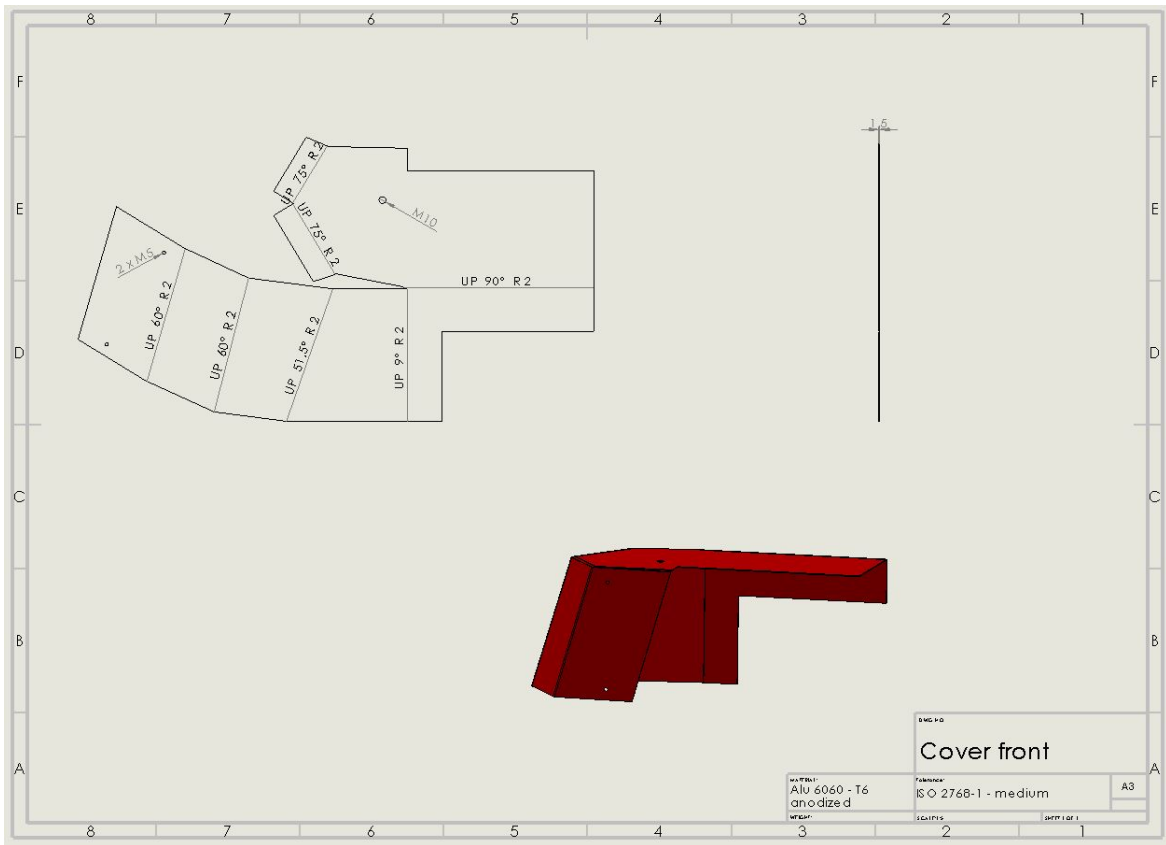


Figure 12-4: Construction drawing of the front cover

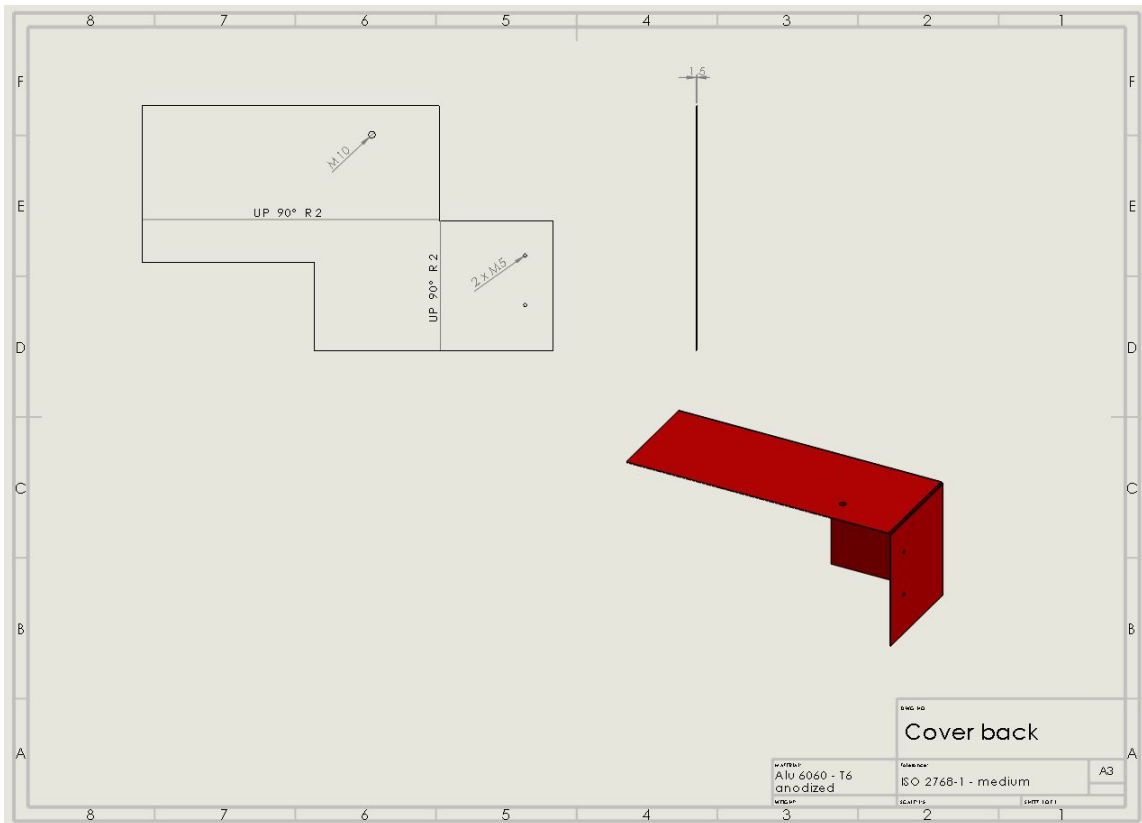


Figure 12-5: Construction drawing of the back cover

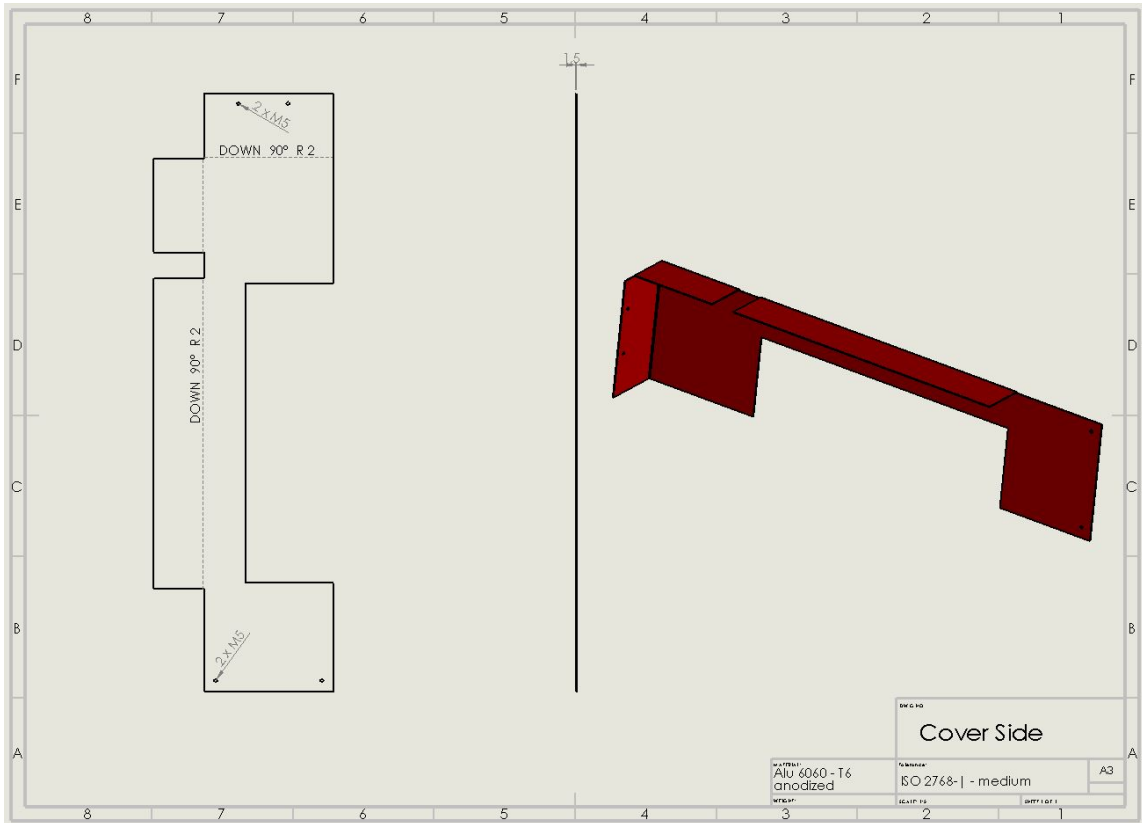


Figure 12-6: Construction drawing of the side cover

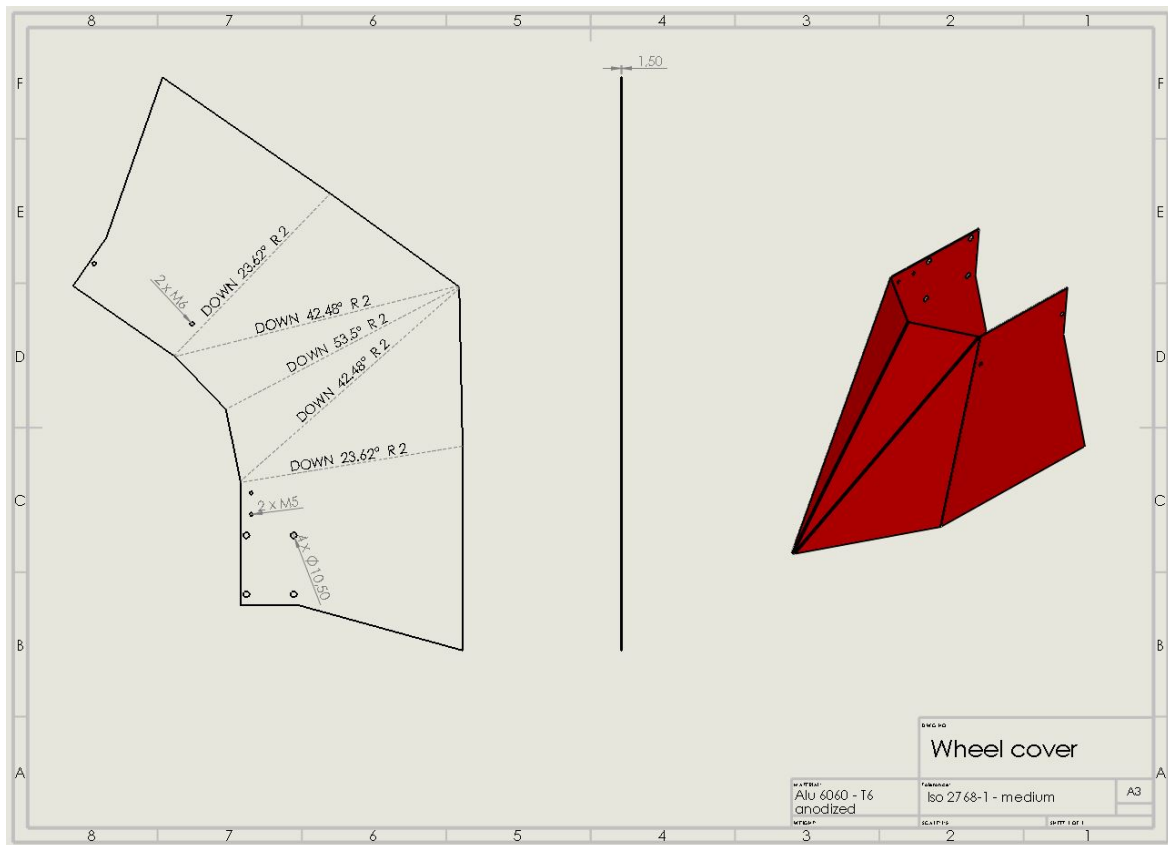


Figure 12-7: Construction drawing of the wheel cover









Norges miljø- og biovitenskapelig universitet  
Noregs miljø- og biovitenskapelige universitet  
Norwegian University of Life Sciences

Postboks 5003  
NO-1432 Ås  
Norway